



DE81030857

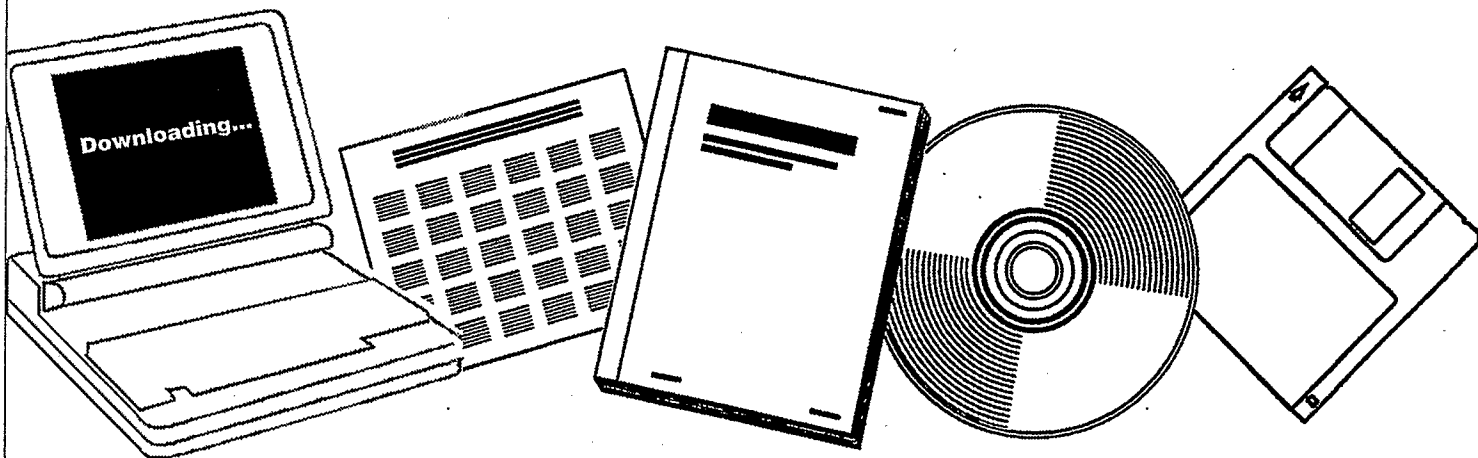
NTIS

One Source. One Search. One Solution.

SYNTHESIS GAS CONVERSION TO LIQUID FUELS USING PROMOTED FUSED-IRON CATALYSTS

DEPARTMENT OF ENERGY, PITTSBURGH, PA.
PITTSBURGH ENERGY TECHNOLOGY CENTER

SEP 1981



U.S. Department of Commerce
National Technical Information Service

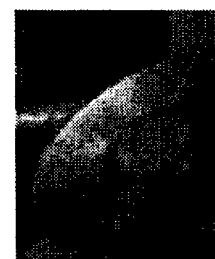
One Source. One Search. One Solution.

NTIS



Providing Permanent, Easy Access to U.S. Government Information

National Technical Information Service is the nation's largest repository and disseminator of government-initiated scientific, technical, engineering, and related business information. The NTIS collection includes almost 3,000,000 information products in a variety of formats: electronic download, online access, CD-ROM, magnetic tape, diskette, multimedia, microfiche and paper.



Search the NTIS Database from 1990 forward

NTIS has upgraded its bibliographic database system and has made all entries since 1990 searchable on **www.ntis.gov**. You now have access to information on more than 600,000 government research information products from this web site.

Link to Full Text Documents at Government Web Sites

Because many Government agencies have their most recent reports available on their own web site, we have added links directly to these reports. When available, you will see a link on the right side of the bibliographic screen.

Download Publications (1997 - Present)

NTIS can now provides the full text of reports as downloadable PDF files. This means that when an agency stops maintaining a report on the web, NTIS will offer a downloadable version. There is a nominal fee for each download for most publications.

For more information visit our website:

www.ntis.gov



U.S. DEPARTMENT OF COMMERCE
Technology Administration
National Technical Information Service
Springfield, VA 22161

DE81030857



DOE/PETC/TR-81/3

(DE81030857)

Distribution Category UC-90d

SYNTHESIS GAS CONVERSION TO LIQUID FUELS

USING PROMOTED FUSED IRON CATALYSTS

Richard A. Diffenbach
Richard R. Schehl
Daniel J. Fauth

CONTENTS

	<u>Page</u>
Summary	3
Background and Objectives	4
Thermogravimetric Results and Discussion	13
Copper and Potassium Promoted Catalysts	14
Molybdenum Promoted Catalysts	27
Microreactor Testing	37
Single Stage	38
On-line	43
Future Studies	50
Bibliography	52
Appendix A Preparation and Composition of Catalysts	53
Appendix B Thermogravimetric Analysis Procedures	55
Appendix C Microreactor Testing Procedures	60

ILLUSTRATIONS

	<u>Page</u>
Figure	
1. Possible Routes to High Octane Gasoline Using Nitrided Iron Catalysts	5
2. Fe-N Phase Diagram	7
3. Iron Nitride Crystal Structure	8
4. Effect of Initial Nitrogen Content of Catalyst on Alcohol and Olefin Production	10
5. Effect of Initial Nitrogen Content of Catalysts on Distribution of Products	11
6. Effect of Initial Nitrogen Content on Oxidation of Catalyst During Synthesis	12
7. Reduction of 200/325 Mesh Fused Iron Oxide Catalysts by H ₂ at 375 ^o C	15
8. Carbiding of 200/325 Mesh Fused Iron Catalysts by CO at 240 ^o C	17
9. Decomposition of Carbide of 200/325 Mesh Fused Iron Catalysts by H ₂ at 450 ^o C	18
10. Nitriding of 200/325 Mesh Fused Iron Catalysts by NH ₃ at 225 ^o C	19
11. Decomposition of Nitride of 200/325 Mesh Fused Iron Catalysts by H ₂ at 200 ^o C	21
12. Reduction of 3½/7 Mesh Fused Iron Oxide Catalysts by H ₂ at 450 ^o C	22

	<u>Page</u>
13. Carbiding of $3\frac{1}{2}/7$ Mesh Fused Iron Catalysts by CO at 250°C	23
14. Decomposition of Carbide of $3\frac{1}{2}/7$ Mesh Fused Iron Catalysts by H_2 at 450°C	24
15. Nitriding of $3\frac{1}{2}/7$ Mesh Fused Iron Catalysts by NH_3 at 350°C	25
16. Decomposition of Nitride of $3\frac{1}{2}/7$ Mesh Fused Iron Catalysts by H_2 at 200°C	26
17. Reduction of 200/325 Mesh Fused Iron Catalysts as a Function of Temperature	28
18. Reduction of Ammonium Molybdate by H_2	29
19. Rates of Nitride Formation and Nitride Decomposition	30
20. Decomposition of Fe_2N in He	33
21. Reaction of Iron Nitrides with H_2 at 175°C	35
22. Reaction Sequence Involving Interaction of MoO_3 with Al_2O_3	41
23. Gas Chromatogram of Fischer-Tropsch Product	45
24. Anderson-Schulz - Flory Plot	46
25. Thermogravimetric Balance	56
26. $\text{Fe}_3\text{O}_4 \rightarrow \text{Fe} \rightarrow \text{Fe}_x\text{N}_y$ Transformation	58
27. Microreactor Unit	61
28. Reactor	62
29. Gas Chromatograph Configuration	63
30. Synthesis Gas Reactor Unit	64

TABLES

	<u>Page</u>
1. Standard Heats of Formation ($-\Delta H^{\circ}$) for the Reaction $\text{X}_2 + 2\text{NM} \leftrightarrow 2\text{M}_\text{N}\text{X}$	13
2. Chemisorption of Reduced Fused Iron Catalysts	32
3. Single Stage Microreactor Test Data	38
4. Conversion Data Summary - Mo Promoted vs. Unpromoted Catalysts	37
5. G. C. Analysis - Aqueous Layer	42
6. Retention Times for Compounds Detected by TCD	47
7. Retention Times for Compounds Detected by FID	48
8. Change in Average Degree of Polymerization with Time	49
9. Change in Hydrocarbon Distribution with Time	49
10. Catalyst Composition and Method of Preparation (200/325)	53
11. Catalyst Composition and Method of Preparation ($3\frac{1}{2}/7$)	54

SUMMARY

This study was carried out with the objective of preparing more active and stable nitrided iron catalysts for the conversion of synthesis gas to a product with a high alcohol content that could be used directly as an automotive fuel or converted to a gasoline-like product over a shape selective zeolite in a dual reactor unit.

The rationale is given for the preparation of a molybdenum-promoted nitrided fused iron catalyst. Catalyst characterization yielded equivocal results as to whether a mixed Fe-Mo nitride was formed. Regardless of the nature of the Mo-containing species, these catalysts were significantly more active than unpromoted nitrided fused iron catalyst.

Characterization of fused iron catalysts using thermogravimetric analysis indicated the rates of reduction, carburization, and nitriding were strongly dependent on reaction temperature and particle size as well as the nature of the promoter. X-ray diffraction measurements indicated the metal crystallite size of the reduced catalysts was strongly dependent on reduction temperature.

A microreactor unit capable of on-line gas chromatographic analysis was constructed for the screening of a variety of carbided iron catalysts. The carbon number distribution obtained using a carbided fused iron catalyst was found to correlate with the Anderson-Schluz-Flory equation.

Background and Objectives

This report describes the effort in the Synthesis Gas Chemistry Branch at PETC to develop a more stable and active iron nitride catalyst for the conversion of synthesis gas to a high octane gasoline. This study was an extension of the work carried out by R. B. Anderson and coworkers at the Bureau of Mines in the 1950's and early 1960's(1). While the indirect liquefaction of coal has attained considerable prominence since the 1973 OPEC oil price increase, nitrated iron catalysts, in particular, have received little attention. Yet, the extensive amount of work done by the Bureau of Mines researchers led to the successful testing of iron nitride catalysts in a variety of pilot plant reactors for periods as long as 3000 hours(2,3).

Two routes to high octane gasoline using nitrated iron catalysts were investigated. Our attention centered on Route A (Figure 1), which involved the conversion of a $H_2 + CO$ synthesis gas over iron nitride to give an aqueous layer containing primarily C_1-C_3 alcohols and an organic layer containing a mixture of alcohols, olefins, and alkanes. The basis for our interest in nitrated iron catalysts was its high selectivity for alcohol formation. The alcohol selectivity for a typical carbided catalyst was only 20-25% of that found for a nitrated catalyst. Figure 1 shows one possible refining scheme in which the C_1-C_3 alcohols are obtained by distillation of the aqueous layer. The organic fraction was passed over bauxite, which results in the conversion of alcohols to internal olefins. This product is then mixed with the light alcohols to give a high octane gasoline.

Another route is shown in which the product from the first reactor is fed to a second reactor containing ZSM-5 or some other shape-selective zeolite. This route

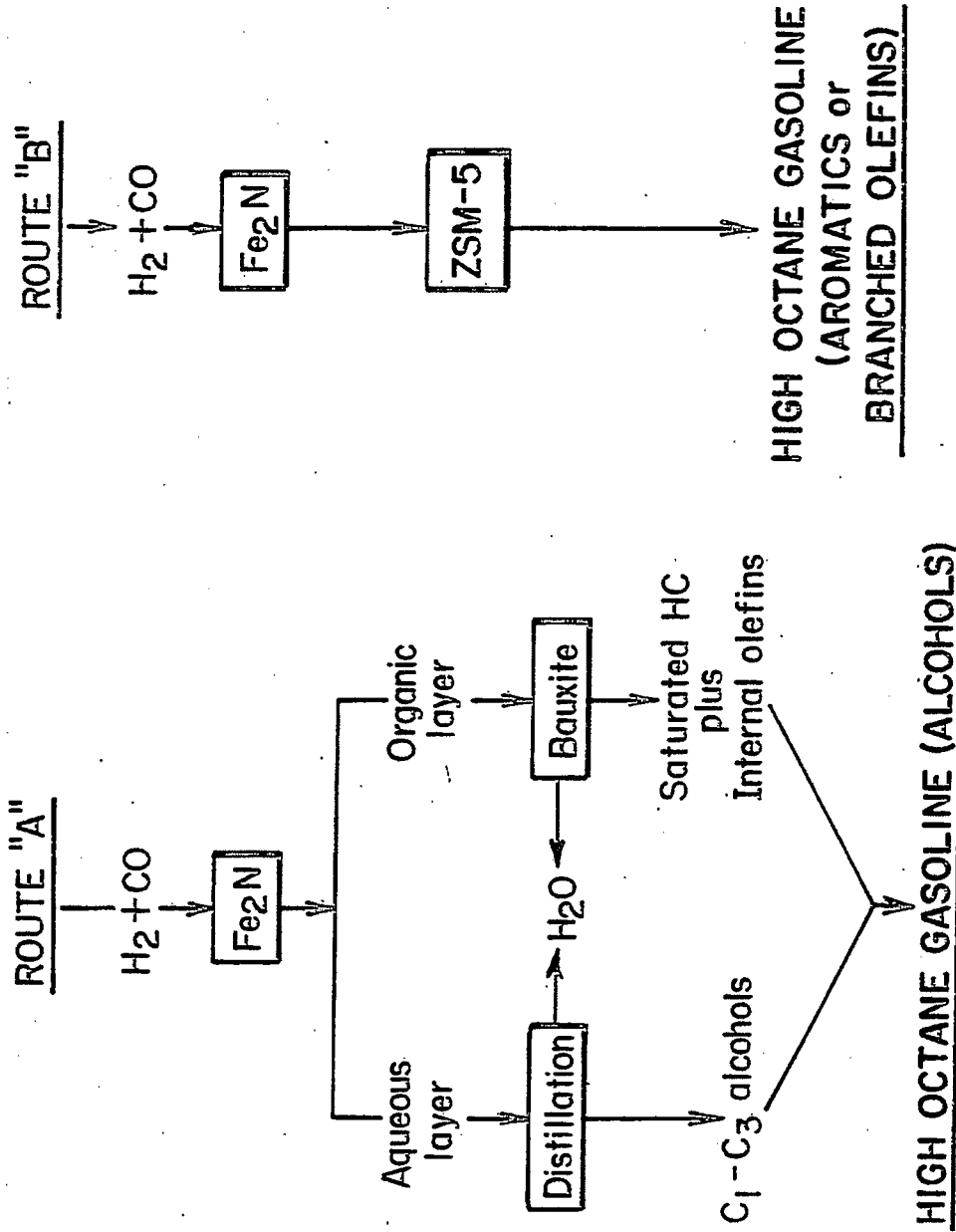


Figure 1-Possible routes to high octane gasoline using nitrided iron catalysts .

L-17655

would be a modification of the Mobil methanol-to-gasoline process (4), insofar as the higher alcohols, as well as methanol, can be converted to C_6-C_{11} aromatics using zeolite catalysts. There is also reason to believe that much of the olefinic product formed using a nitrided iron catalyst can also be converted to an aromatic product.

The iron nitride catalyst was prepared in the following manner: Fused iron oxide catalyst, Fe_3O_4 , also known as magnetite, was reduced to metallic iron; ammonia was then passed over the reduced iron to give a mixture of $\epsilon-Fe_2N$ and $\delta-Fe_2N$. The composition of the catalyst was that predicted by the Fe-N phase diagram (Figure 2). A fully nitrided sample contained about 10 wt.% N, and x-ray diffraction analyses indicated it to be a mixture of $\epsilon-Fe_2N$ and $\delta-Fe_2N$.

Iron nitride is a member of a group of compounds known as interstitial compounds. The term traditionally refers to combinations of relatively large transition metals such as Mo, Fe, Cr, Co, Ni, V, and Mn with the small metalloids such as H, B, C, and N. The structure of $\epsilon-Fe_2N$ is shown in Figure 3(5).

Our analysis of the Bureau of Mines data indicated that the major problem involved with the use of an iron nitride catalyst was the following: at the conditions used for synthesis gas conversion -- $H_2 + CO$ synthesis gas, $220^{\circ} - 250^{\circ}C.$ and 300 psig -- the nitrogen atoms in iron nitride were slowly replaced by carbon atoms so that the high selectivity found initially for alcohol formation decreased over a period of time. Eventually, if a sufficient number of nitrogen atoms were replaced, the product selectivity resembled that found for carbided iron catalyst, namely, low alcohol selectivity and more heavy oil and wax.

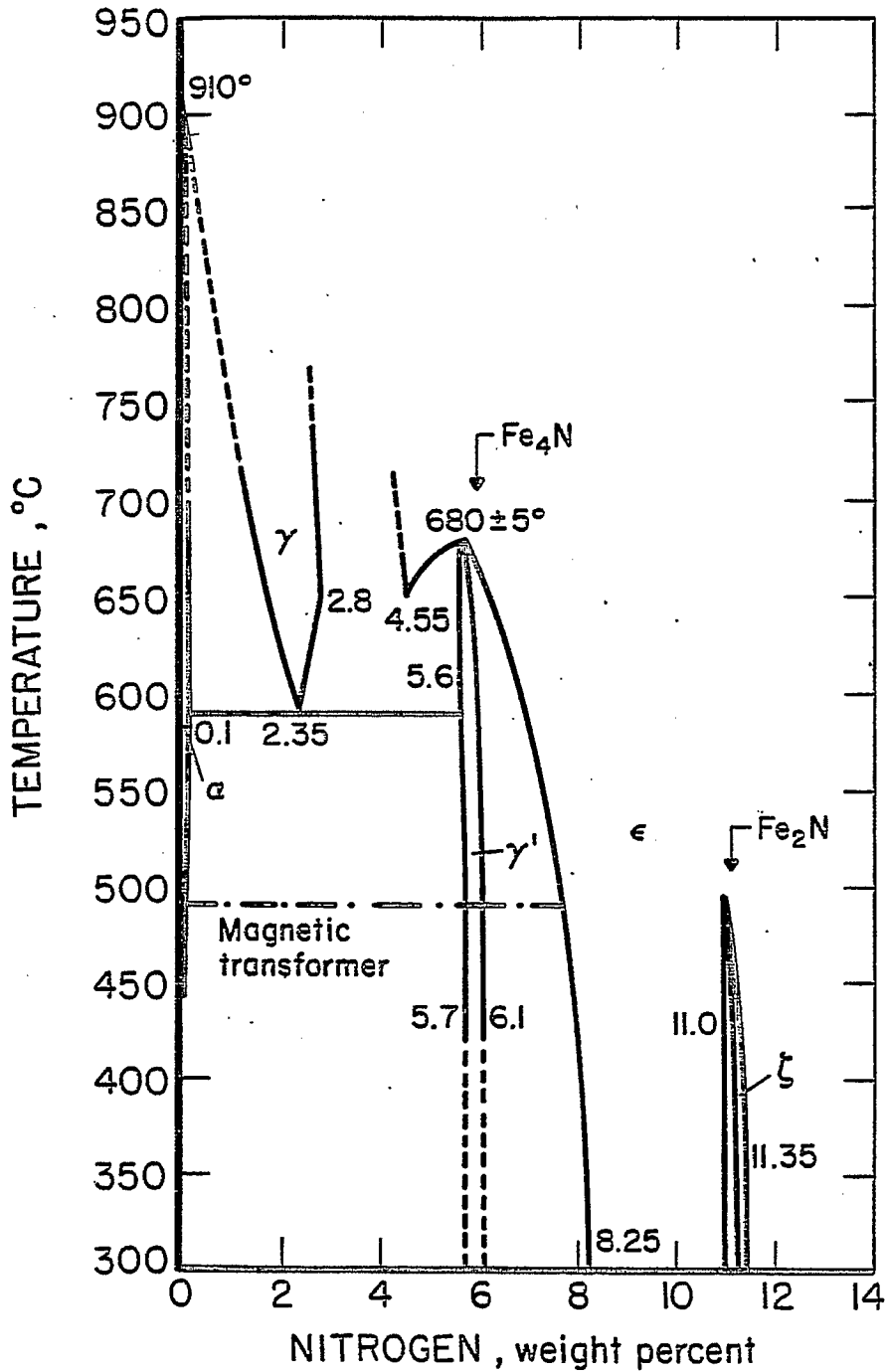


Figure 2 - Fe-N PHASE DIAGRAM

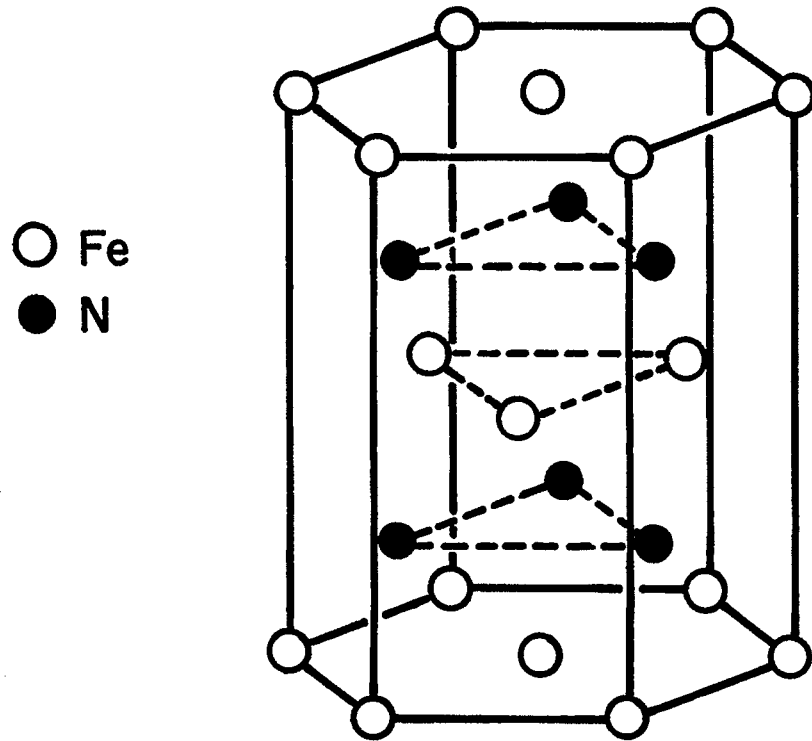


Figure 3 - Iron nitride crystal structure.

5-5-80 L-17644

A portion of the Bureau of Mines data is reviewed in Figures 4-6(1). Reduced iron catalysts were nitrated to varying degrees, with N/Fe atom ratios ranging from 0 (no nitriding) to about 0.45 (fully nitrated). Figure 4 indicates there was a sharp decrease in alcohol selectivity with lesser degrees of nitriding. At the same time there was a corresponding increase in the selectivity for α -olefins, which suggested that alcohols were the primary reaction product and subsequently underwent dehydration to the corresponding olefin. Figure 5 indicates that as the degree of nitriding decreased, there was a significant decrease in the selectivity for the gasoline fraction (27^o - 185^oC) and at the same time an increase in the amount of heavy oil and wax. The importance of the N/Fe ratio is again shown in Figure 6. Nitrated iron catalysts oxidized far less rapidly than the corresponding carbided catalyst, resulting in maintenance of the high initial activity of nitrated catalysts for longer periods. Unless these catalysts are studied at very low CO conversions, the partial pressures of steam and CO₂ in the reactor are sufficiently high for the thermodynamics to favor oxidation of the metallic iron as well as the iron carbide.

The objective of the research effort described in this report was to prepare a more stable iron nitride catalyst that would minimize the conversion of the nitride to the carbide. Fortunately, a considerable amount of thermodynamic data was available on the stability of various metal oxides, carbides, and nitrides (6). If the assumption is made that the ΔS° values are nearly the same for a class of compounds (nitrides or oxides or carbides), then the ΔH° values shown in Table I are indicative of the stability of these compounds.

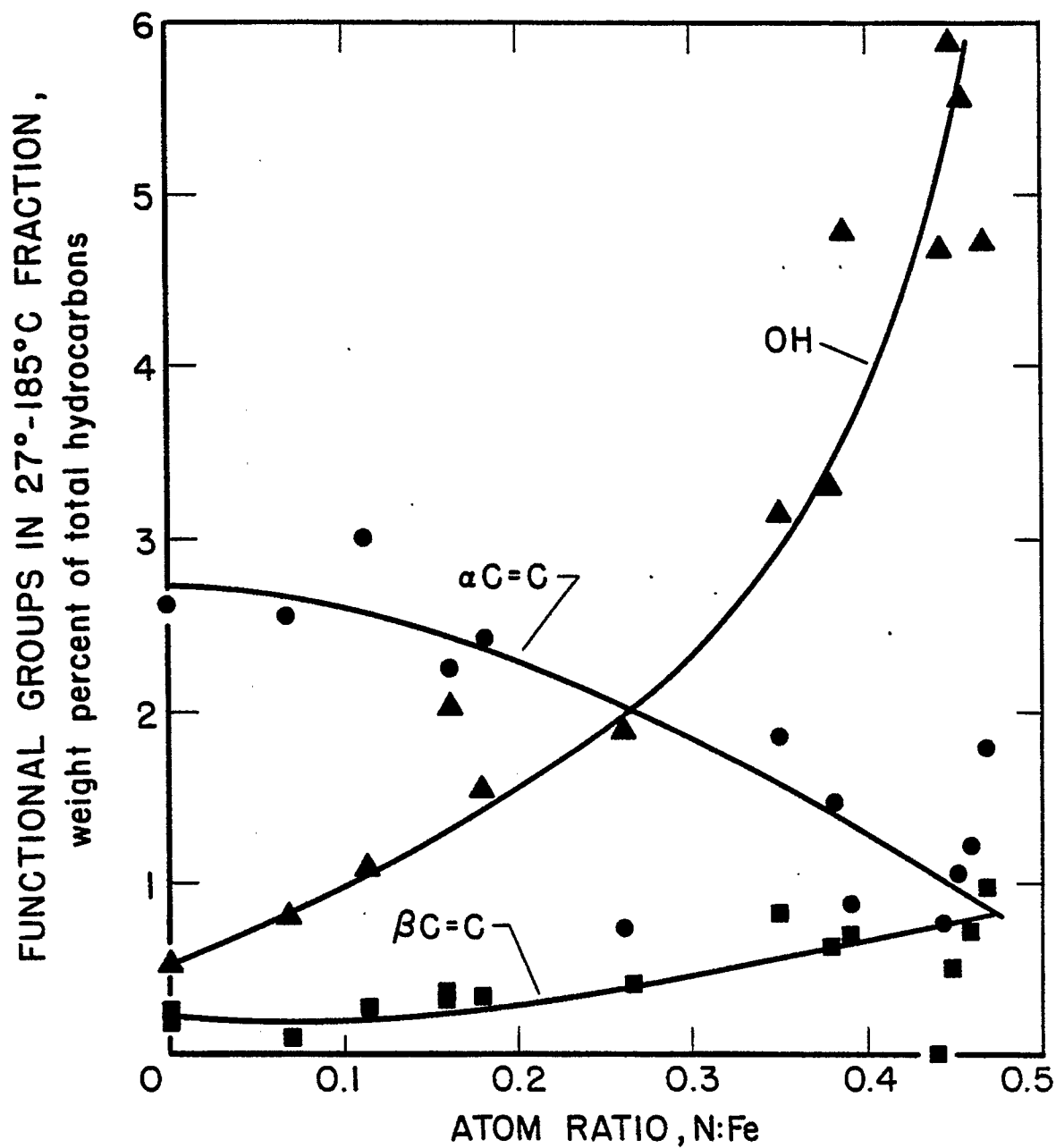


Figure 4 - Effect of initial nitrogen content of catalyst on alcohol and olefin production .

5-5-80 L-17638

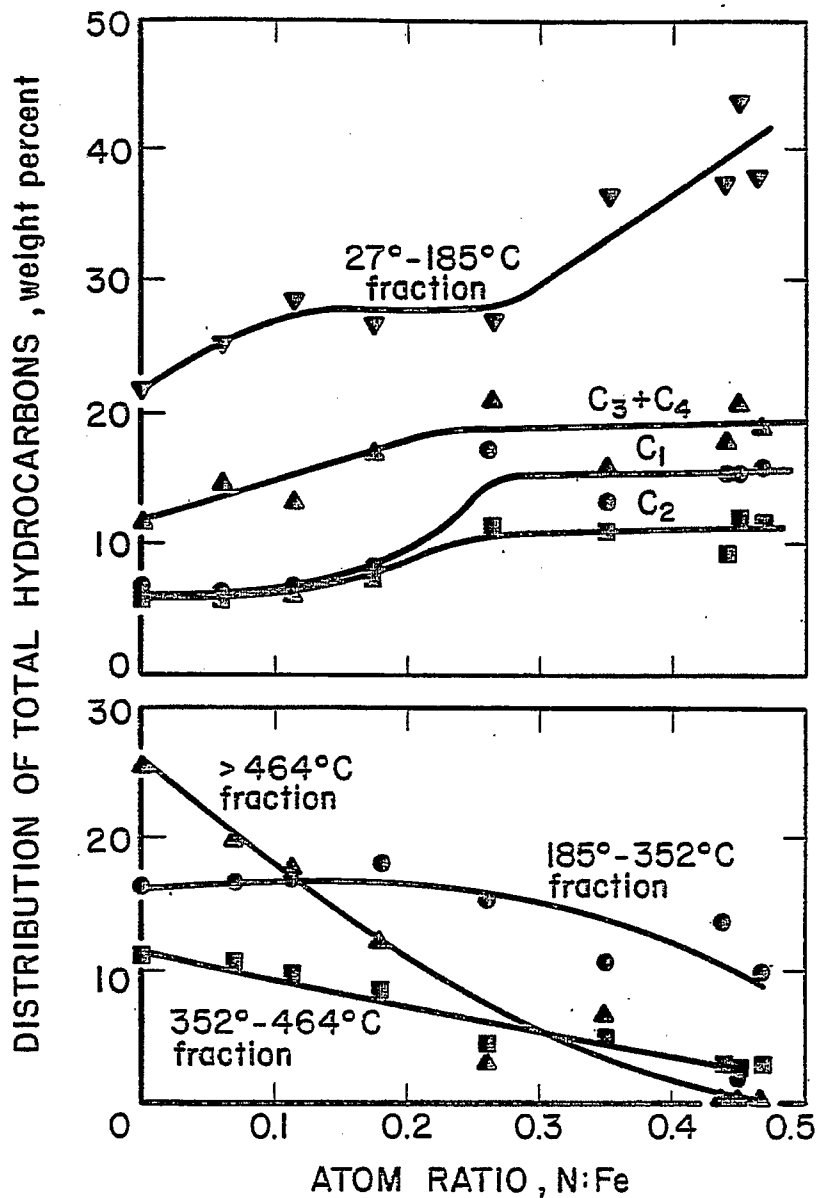


Figure 5 - Effect of initial nitrogen content of catalysts on distribution of products. Total hydrocarbons includes oxygenated material dissolved in liquid phase.

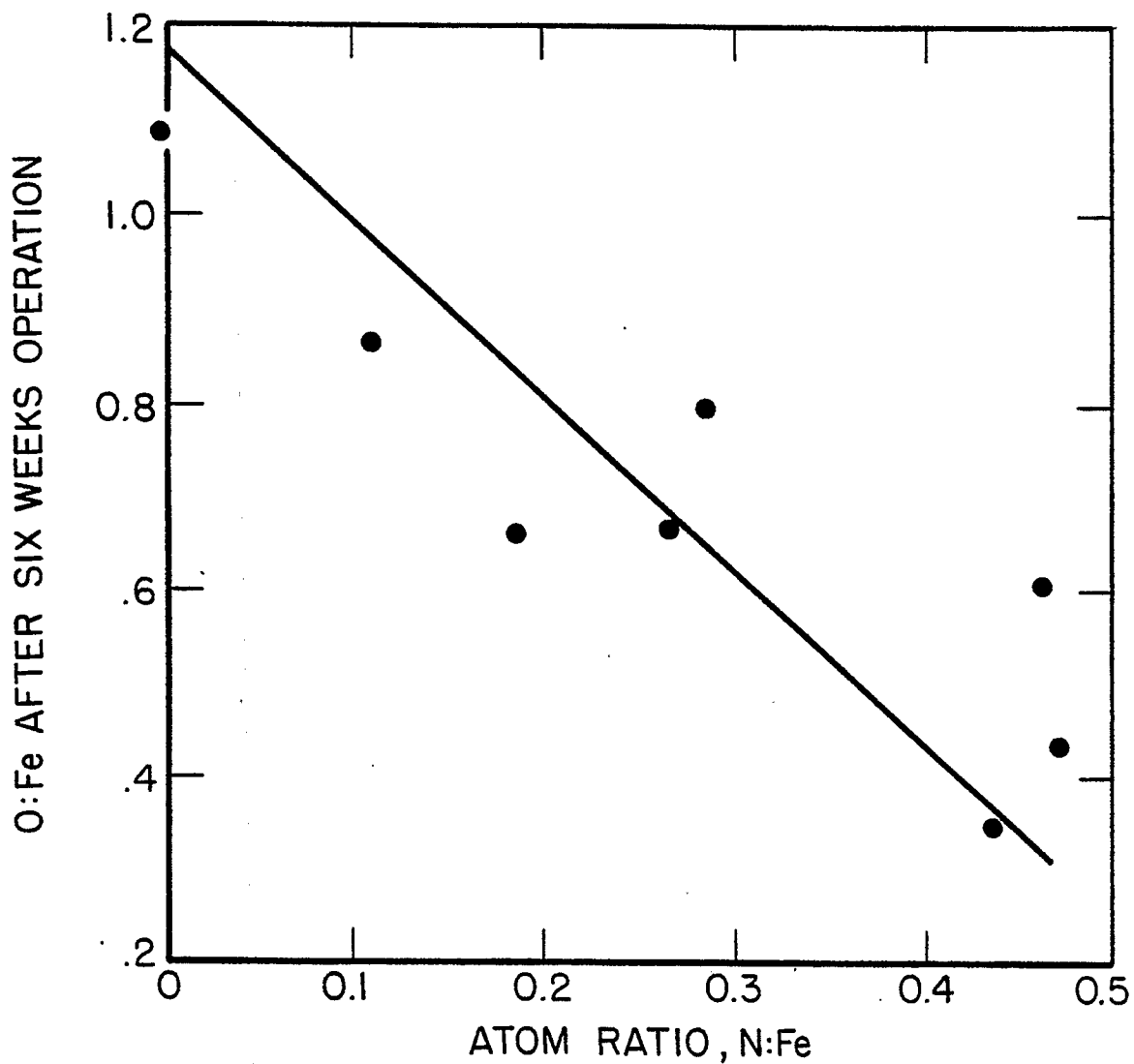


Figure 6- Effect of initial nitrogen content on oxidation of catalyst during synthesis.

5-5-80 L-17639

TABLE I
STANDARD HEATS OF FORMATION ($-\Delta H^0$) FOR THE REACTION



Cr ₂ O ₃ 90	MnO 90	Fe ₂ O ₃ 66	CoO 51	NiO 58	CuO 37
Cr ₂ N 27	Mn ₄ N 31	Fe ₄ N 3	Co ₃ N -2	Ni ₃ N 0	Cu ₃ N -18
Cr ₃ C ₂ 3	Mn ₃ C 4	Fe ₃ C -5	Co ₃ C -4	Ni ₃ C -9	Cu ₃ C unstable
MoO ₃ 60		RuO ₂ 36	RhO 22	PdO 23	Ag ₂ O 7
Mo ₂ N 17					
MoC 3					
		OsO ₂ 31	Ir ₂ O ₃ 27		Au ₂ O ₃ 0.3

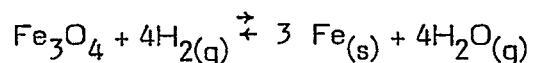
It is apparent that Mo, Cr, and Mn all form nitrides far more stable than iron. Since data accumulated in the latter stages of this study indicated chemical reactivity of the nitrides towards hydrogen or carbon monoxide was the important factor in determining the rate of conversion of iron nitride to the carbide, it may not have been appropriate to use the values in Table I as a guide to select a metal to stabilize iron nitride. The specific objective then was to prepare a mixed metal nitride with increased stability and with a selectivity for alcohols at least equivalent to that of iron nitride alone.

Thermogravimetric Results and Discussion

Data obtained using the thermogravimetric analyzer (T.G.A.) proved to be quite useful in choosing the temperatures to be used for reduction, carburizing, and nitriding in the microreactor tests. In addition, these data provided valuable insight into the mechanism of the promoting action of various metals such as copper, potassium, and molybdenum.

Copper and Potassium Promoted Catalysts

Results of the thermogravimetric studies are shown in Figure 7-16, plotted as percent weight change versus time. Figure 7 shows the reduction of the (200/325)* mesh catalysts by H₂ at 375⁰C, according to the equation:



The catalyst containing 5.2% potassium (#2) displayed a slow rate of reduction compared to the reference (#1) or copper promoted catalysts (#3 and #4). This could be attributed to a number of factors. Firstly, coverage of the catalyst surface by K₂CO₃ may block access of hydrogen or carbon monoxide to the catalyst surface. Secondly, Dry and coworkers (7) have reported that the presence of K₂CO₃ on the catalyst surface increases the heat of adsorption of CO while decreasing that of H₂. If it is assumed that the rate of adsorption of H₂ is the rate-limiting step in the reduction, then the overall rate of reduction would be slower for those catalysts treated with K₂CO₃, provided the rate of H₂ adsorption is proportional to its heat of adsorption.

The reduction rate was markedly increased for copper promoted catalysts. These results were not unexpected since copper salts are readily reduced to metallic copper. Reduction of the iron oxide would then be more facile, since H₂ could spillover from the metallic copper to the iron oxide.

*(200/325) mesh refers to a particle size range in which the particles pass through a 200 mesh screen but sit on a 325 mesh screen.

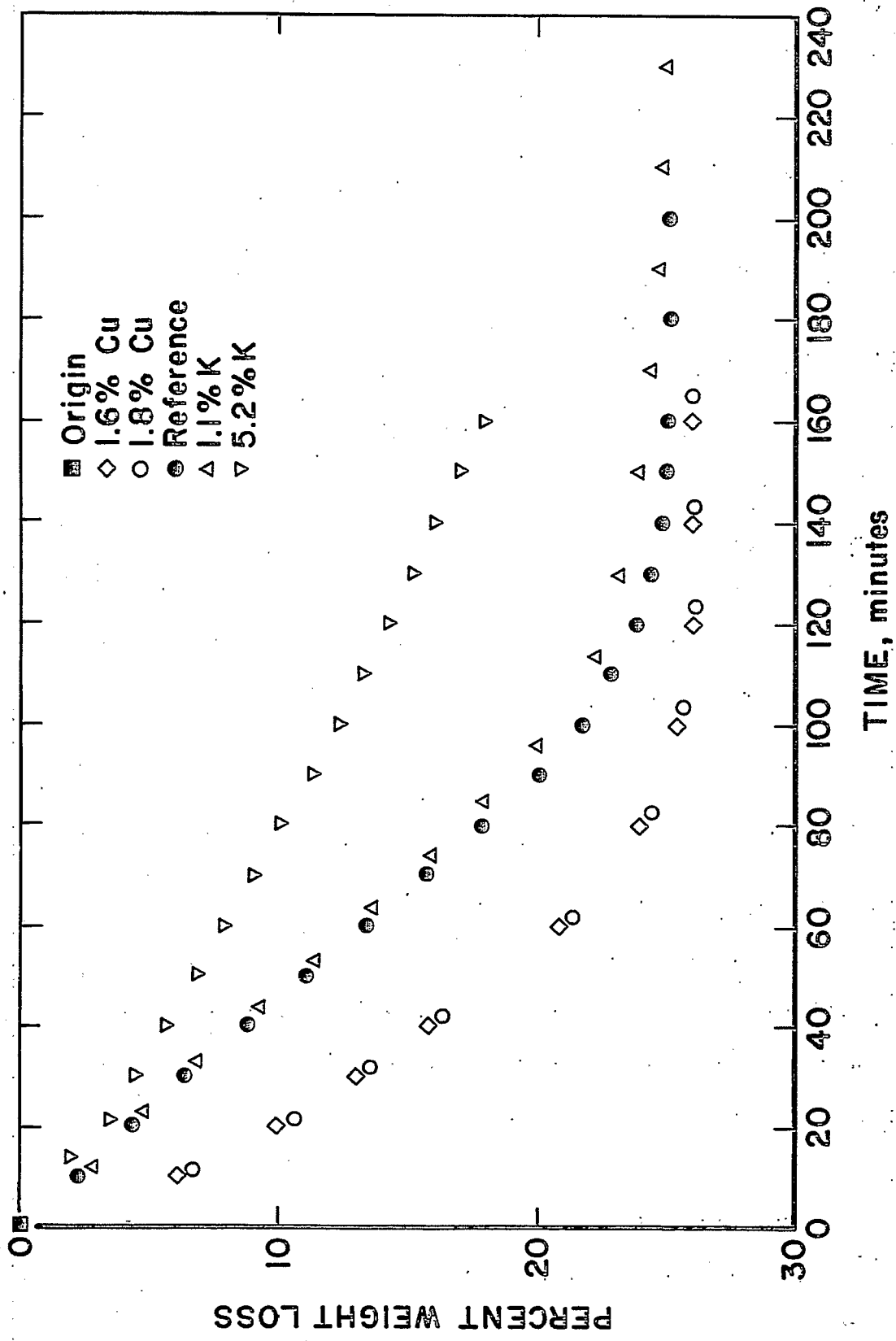
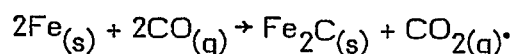


Figure 7 - Reduction of fused iron oxides by H₂ at 375°C

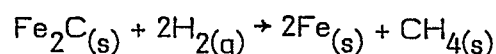
10-16-79 L-17067

Carbiding of these catalysts by carbon monoxide at 240°C is shown in Figure 8. Previous work indicated that the Hagg carbide was likely to be formed under these conditions; the reaction can be approximated by the following equation:



The potassium promoted catalysts carbided the most rapidly; this probably was due to the increased heat of adsorption of CO on K_2CO_3 promoted catalysts mentioned above. The copper promoted catalysts carbided somewhat more slowly than the untreated catalyst. This may have been due to the fact that a substantial portion of the catalyst surface was covered with copper, which does not form a stable carbide.

Figure 9 shows the decomposition of the carbides by H_2 at 450°C. Decomposition probably occurred according to the equation:



Promotion of the catalyst with K_2CO_3 imparted considerable stability to the carbide. Dry's work again would explain this behavior since the presence of K_2CO_3 should decrease the surface coverage by H_2 . In the case of the copper-containing catalysts, spillover of H_2 from the metallic copper to the iron carbide could account for the more rapid decomposition of these catalysts.

Nitriding of the reduced catalysts with NH_3 at 225°C is shown in Figure 10. The reaction occurred according to the equation:

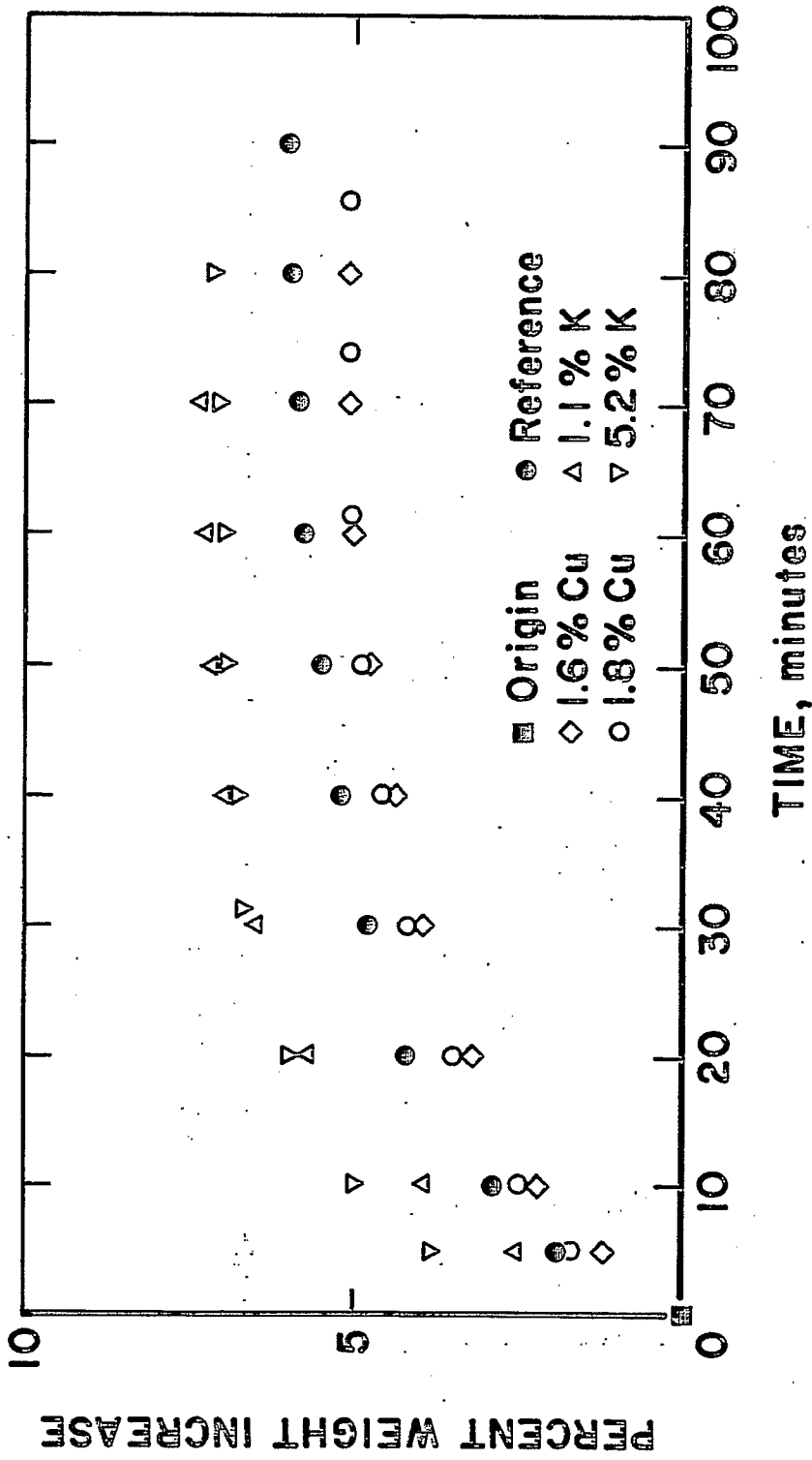


Figure 8 - Carbiding of reduced fused iron catalysts by CO at 240°C

10-16-79 L-17068

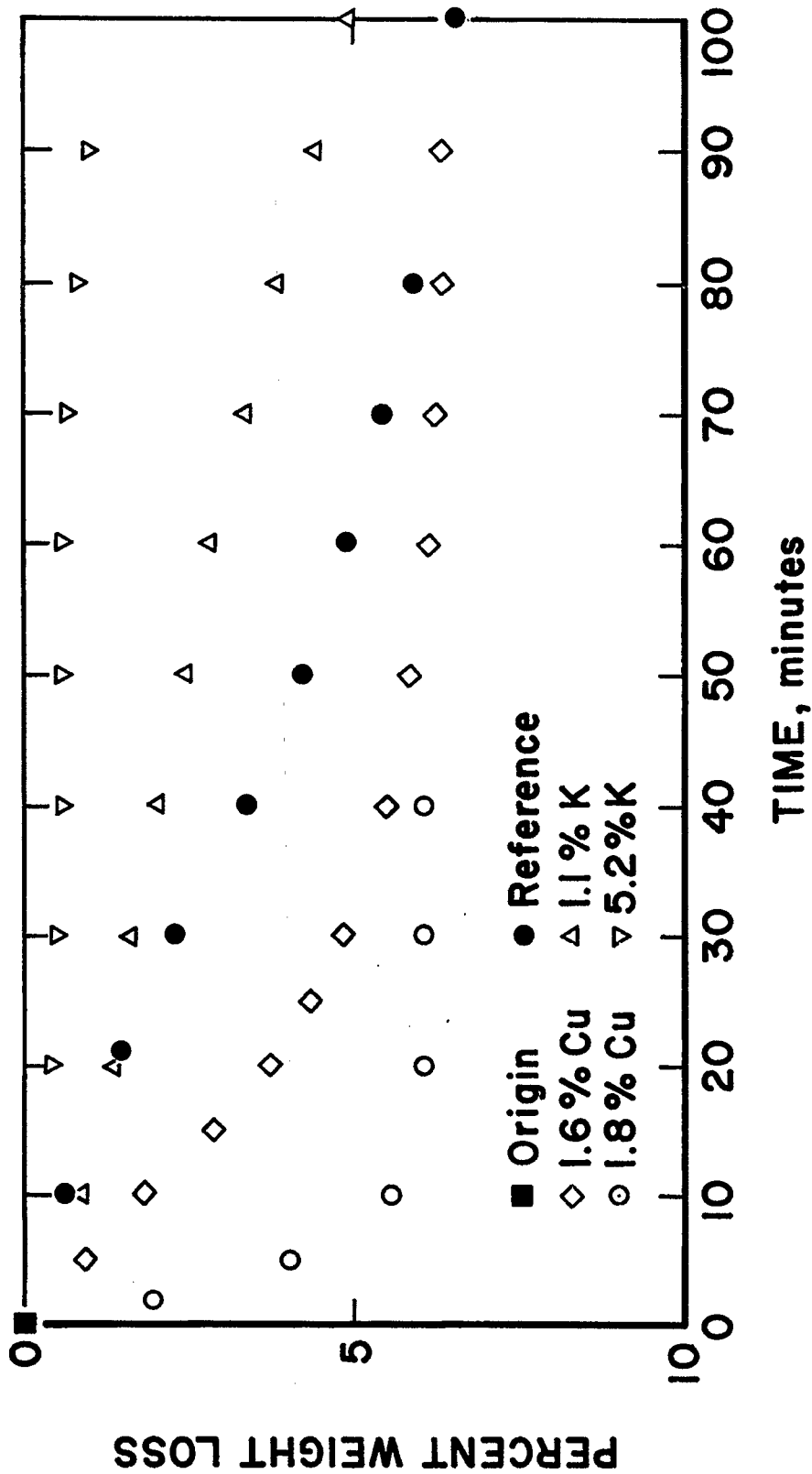


Figure 9 - Decomposition of carbided fused iron catalysts by H₂ at 450°C

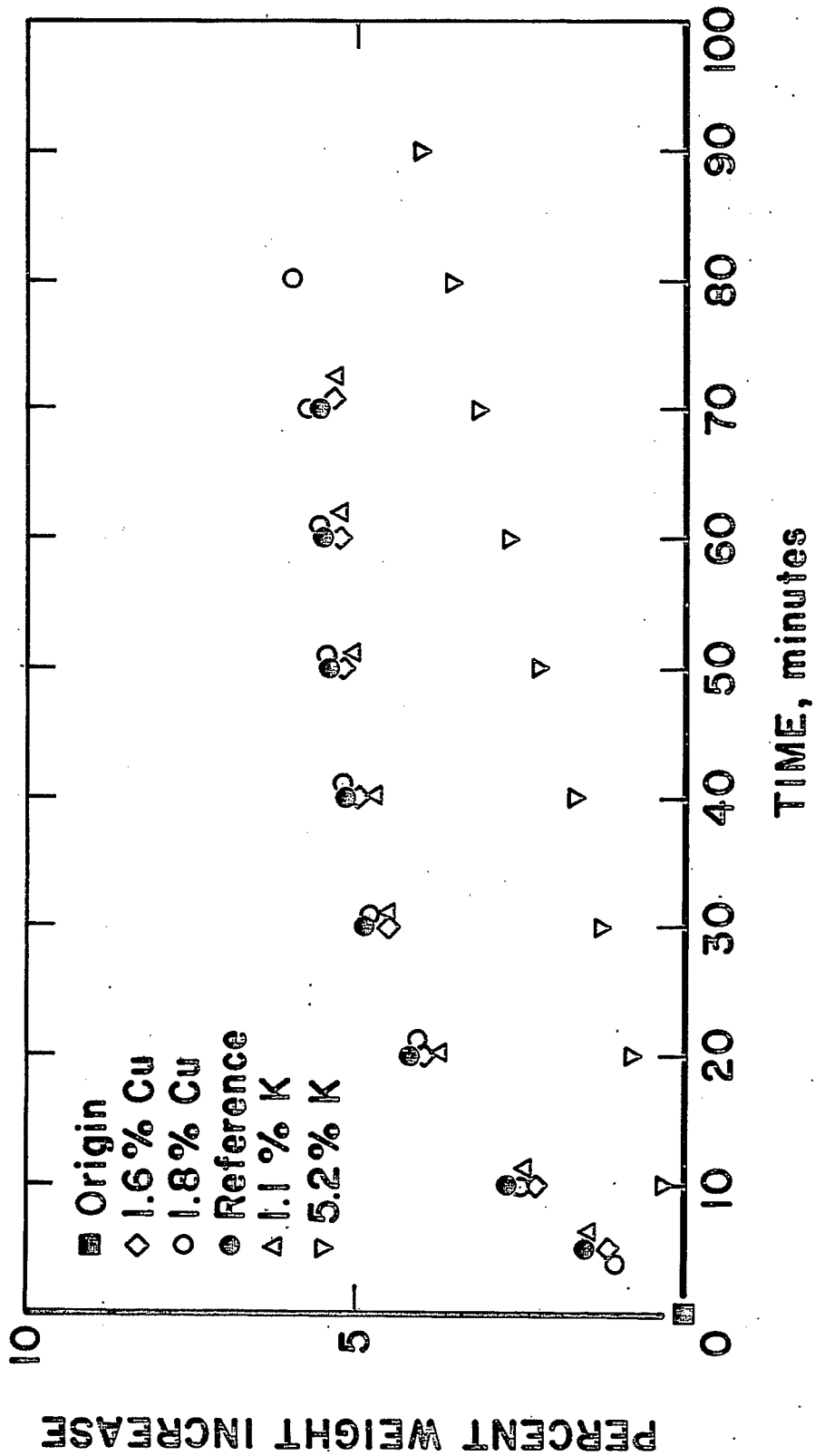
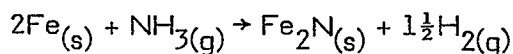


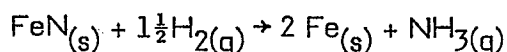
Figure 10-Nitriding of reduced fused iron catalysts by NH₃ at 225°C

10-16-79 L-17070



All of the catalysts showed about the same reactivity except the 5.2% K sample, which nitrided at a considerably slower rate. This again may have been due to blockage of the sites by K_2CO_3 or, if the NH_3 absorbed more rapidly on acidic sites, neutralization of these sites by the basic K_2CO_3 .

Figure 11 shows the decomposition of the nitrides by H_2 at 200°C .



Little difference in reactivity was observed, although this may have been due to the fact that these rates were measured within a temperature range where bulk diffusion of H_2 is the rate limiting step.

Percent weight changes for the $(3\frac{1}{2}/7)$ mesh catalysts are plotted in Figures 12-16. The catalysts studied were as follows:

Catalysts

7	unpromoted
8	1.0% K_2O
9	0.10% Cu

These catalysts are more completely identified in Appendix A. Reduction by H_2 at 450°C and carbiding by CO at 250°C showed essentially identical behavior for all three of the catalysts. The catalysts behaved similarly when the carbides were decomposed by H_2 at 450°C , with the untreated catalyst showing slightly greater stability.

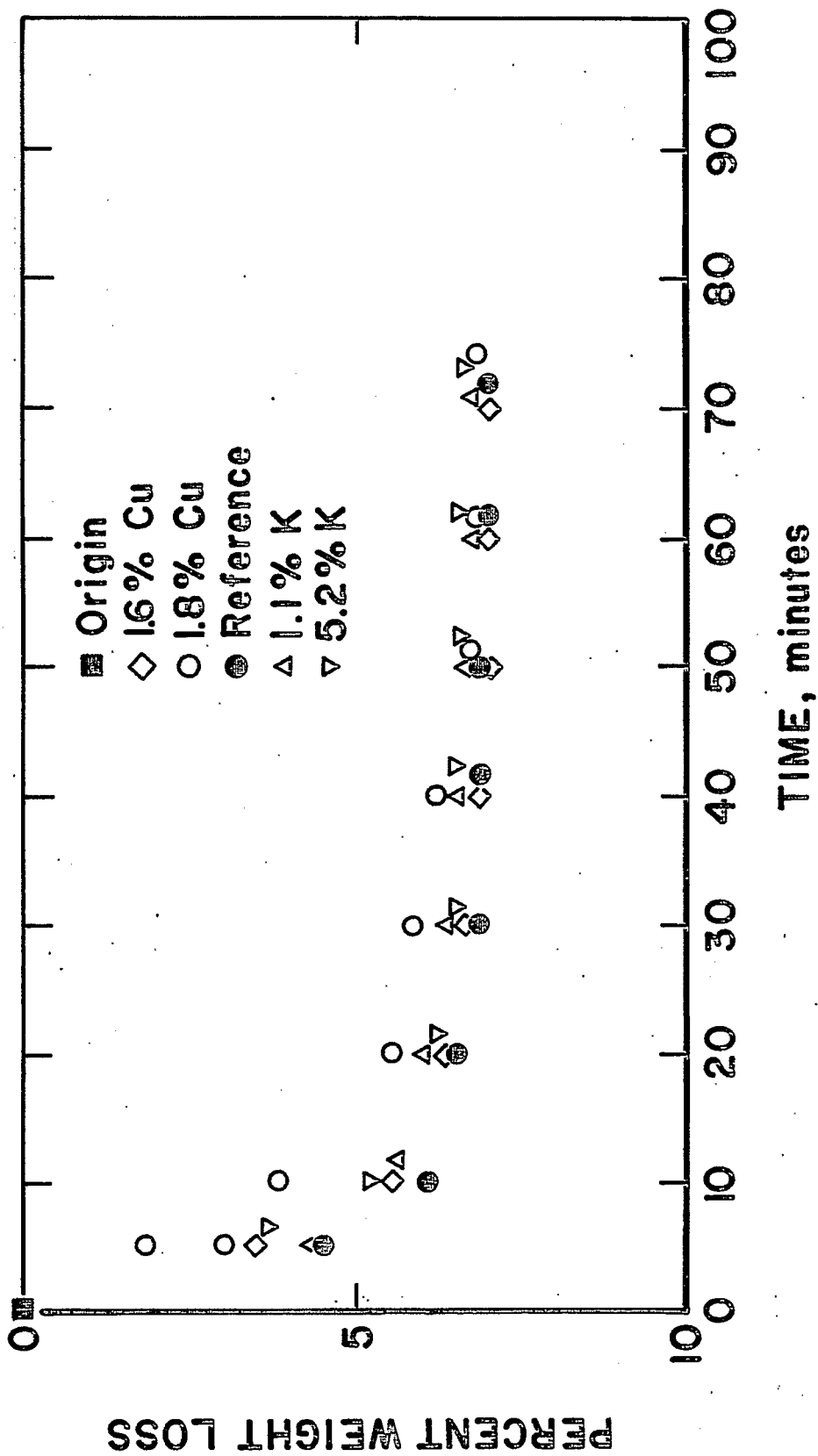


Figure 11 - Decomposition of nitrided fused iron catalysts by H₂ at 200° C

10-16-79 L-17071

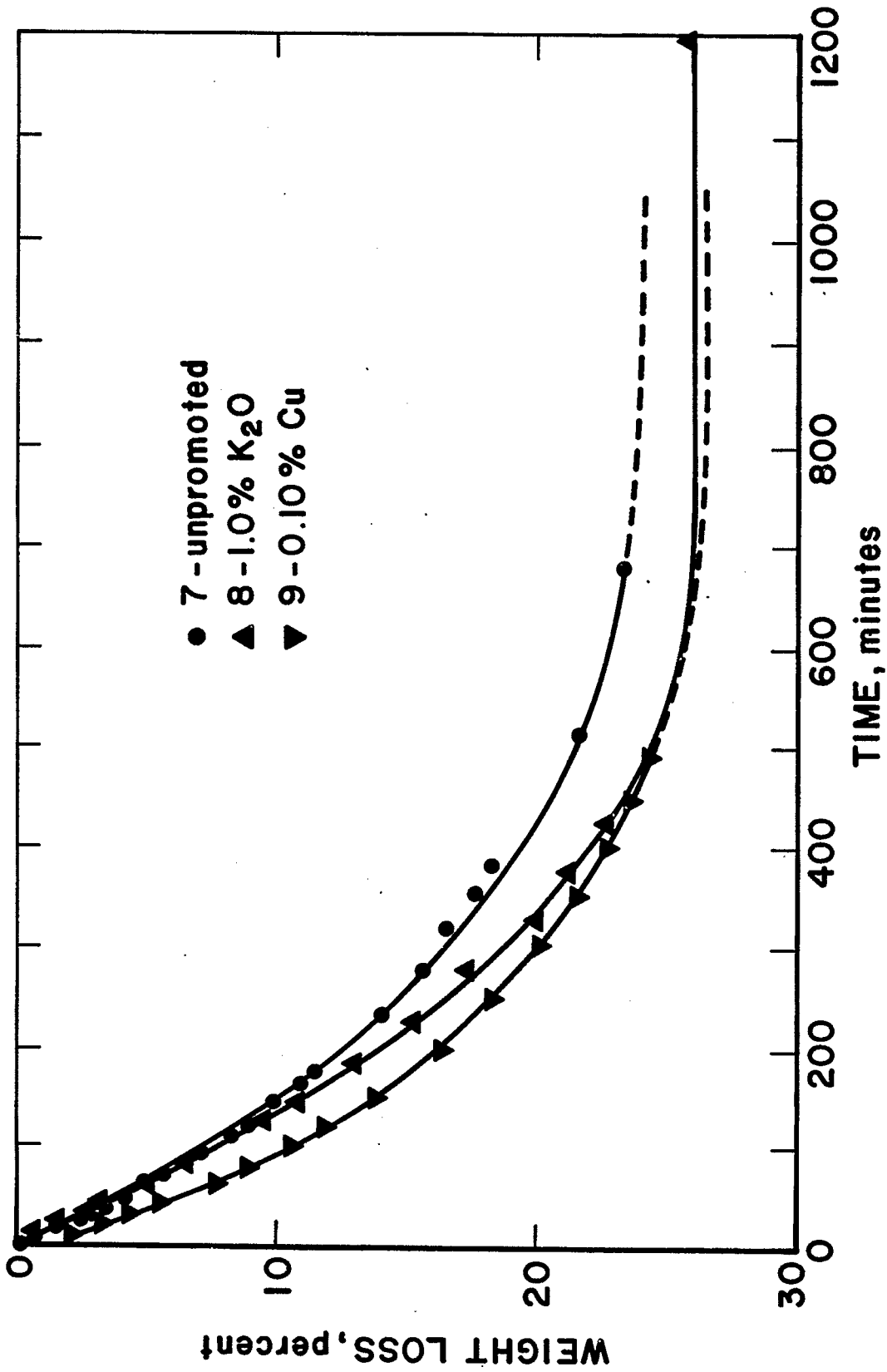


Figure 12 - Reduction of 3¹/₂ / 7 mesh fused - iron oxide catalysts by H₂ at 450°C.

L-81251

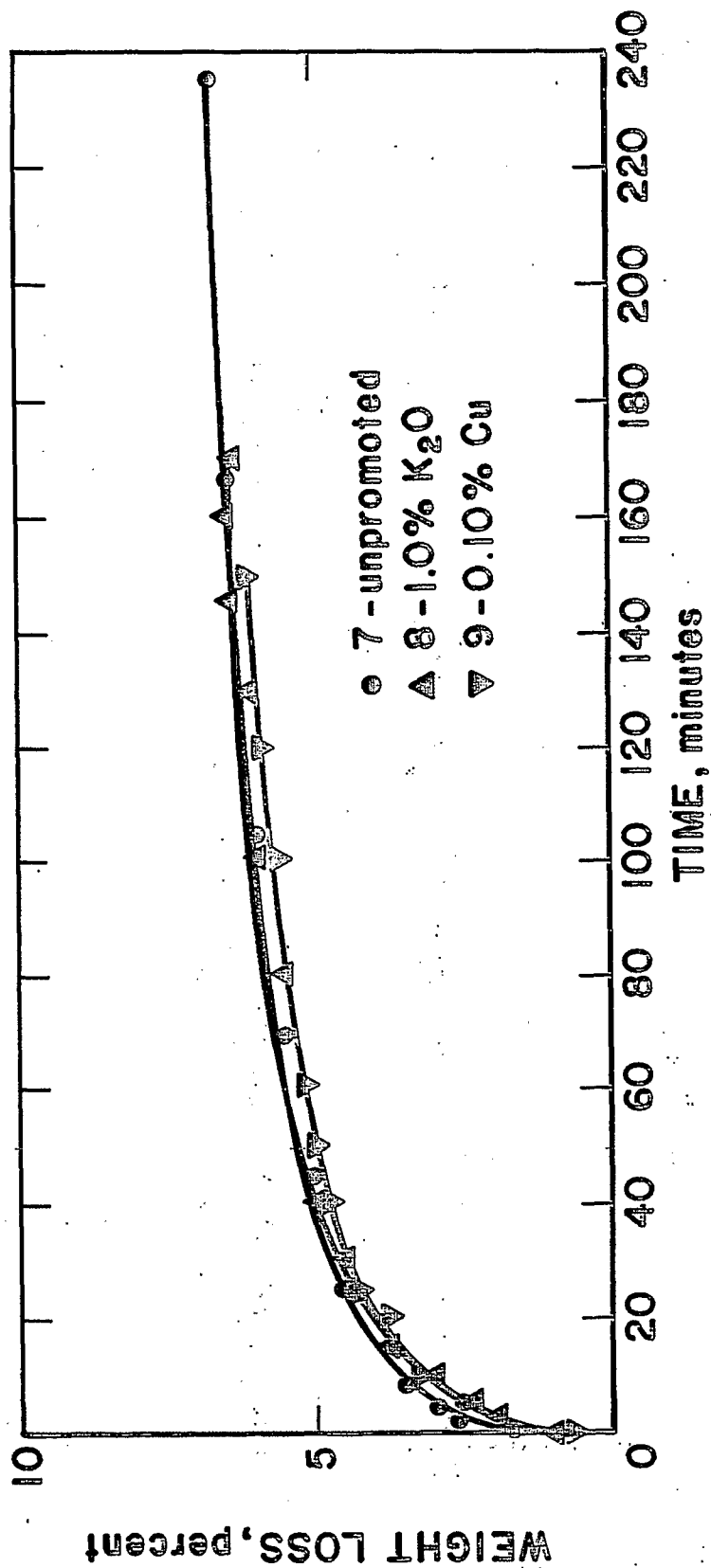


Figure 13 - Carbiding of 3 1/2 / 7 mesh fused -iron catalysts by CO at 250°C.

L-81252

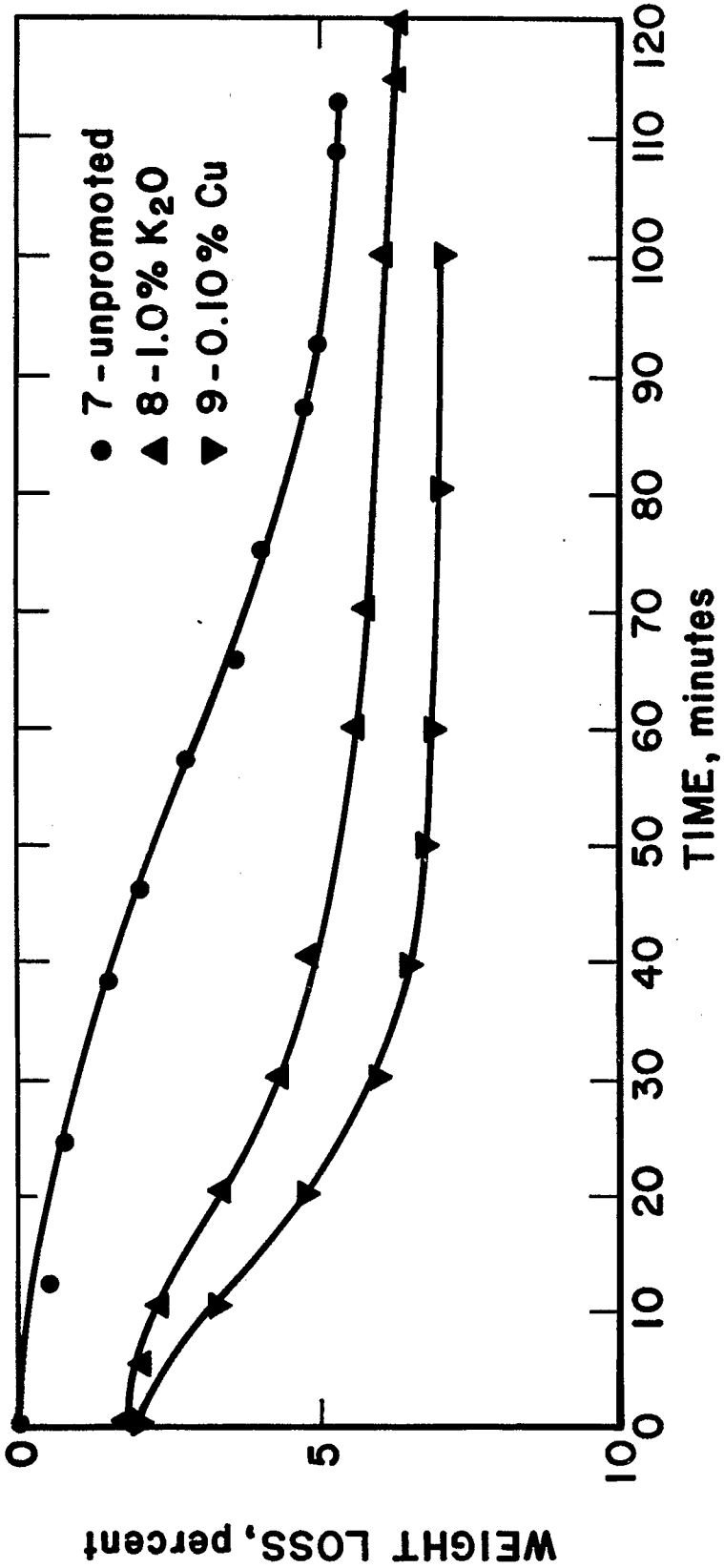


Figure 14 - Decomposition of carbide of 3 1/2 / 7 mesh fused - iron catalysts by H₂ at 450°C .

L-81253

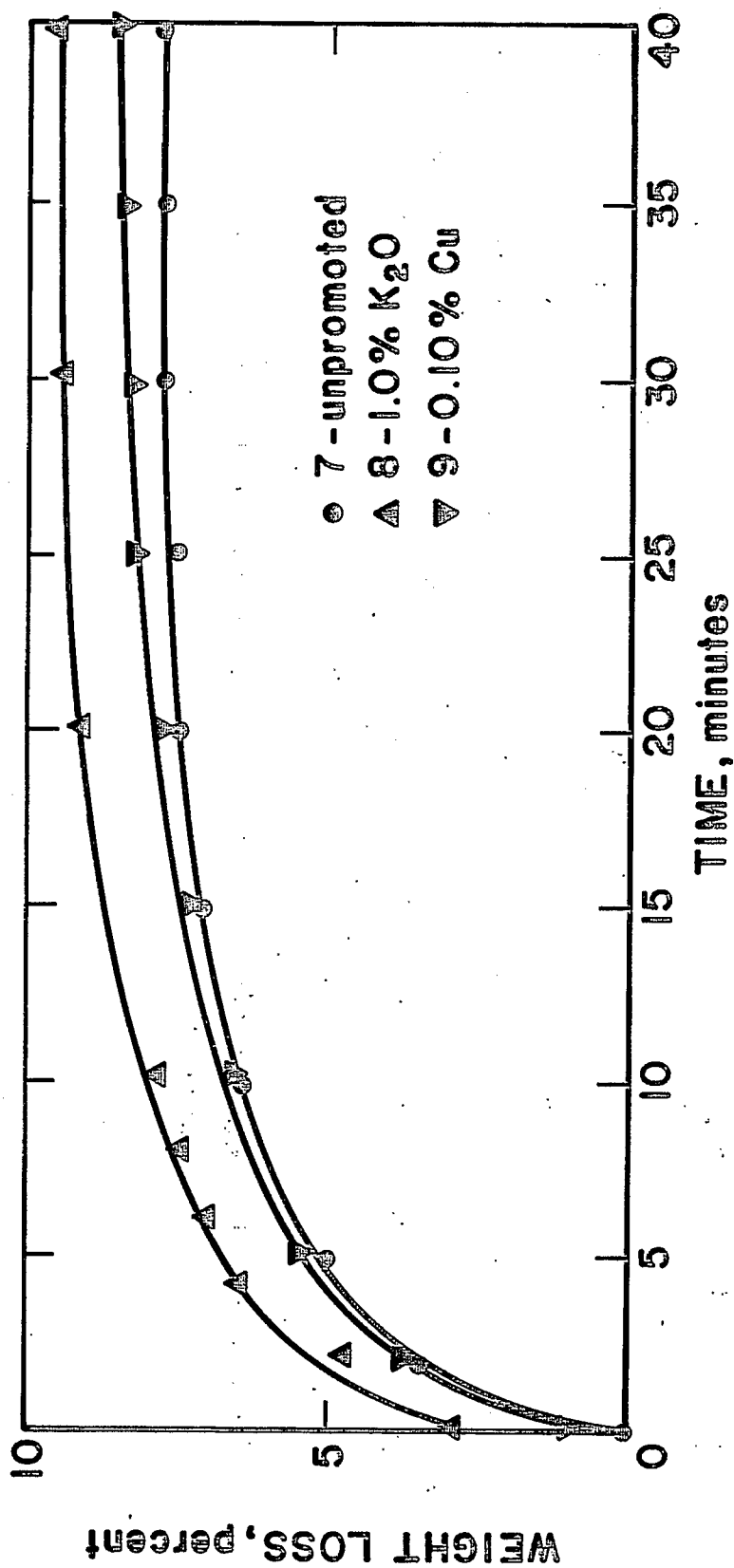


Figure 15 - Nitriding of 3 1/2 / 7 mesh fused - iron catalysts by NH₃ at 350°C.

L-81254

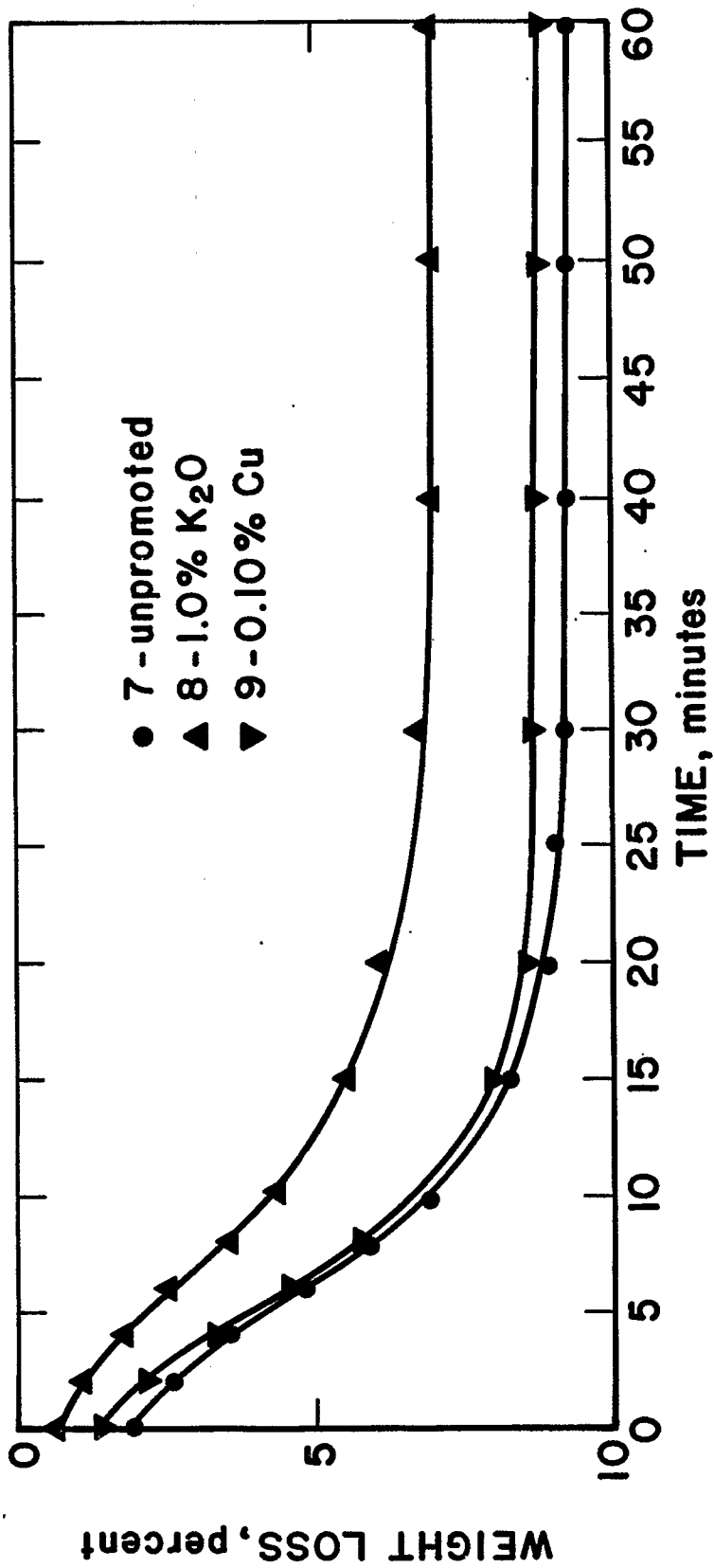


Figure 16 - Decomposition of nitride of 3¹/₂ / 7 mesh fused - iron catalysts by H₂ at 450°C .

L-81255

All of the large particle catalysts again showed practically identical behavior when nitrated by NH_3 at 350°C and decomposed by H_2 at 200°C . The similarity in behavior of these catalysts was probably due to the fact that only small amounts of the promoters were present.

B. Molybdenum Promoted Catalysts

In the microreactor studies, a standard reduction temperature of 450°C was chosen. This temperature was selected as a result of a study of the rate of reduction of the standard catalyst as a function of temperature (Figure 17). While the reduction is essentially complete after one hour at 400°C , standard reduction conditions of 450°C for two hours were chosen. It should be noted however, that a temperature of 375°C or lower would have been sufficiently high if extended reduction periods were used.

As described earlier, one of the objectives of the research described in this report was to prepare a iron-molybdenum nitride catalyst. Figure 18 shows that a considerably higher temperature is required for reduction of ammonium molybdate to molybdenum metal. A temperature of 550°C was required for complete reduction. Even at long reduction periods (up to 24 hours), temperatures of 500°C or less could not effect complete reduction. The reduction of ammonium molybdate, after impregnating a fused iron oxide catalyst, may be more or less facile depending on whether it is associated with reduced iron metal or with alumina found in the catalyst. If the ammonium molybdate is in intimate contact with the iron crystallites, then hydrogen spillover may result in reduction occurring more readily. If compound formation occurs between molybdenum oxide and alumina, however, then even a temperature of 550°C might not be sufficiently high

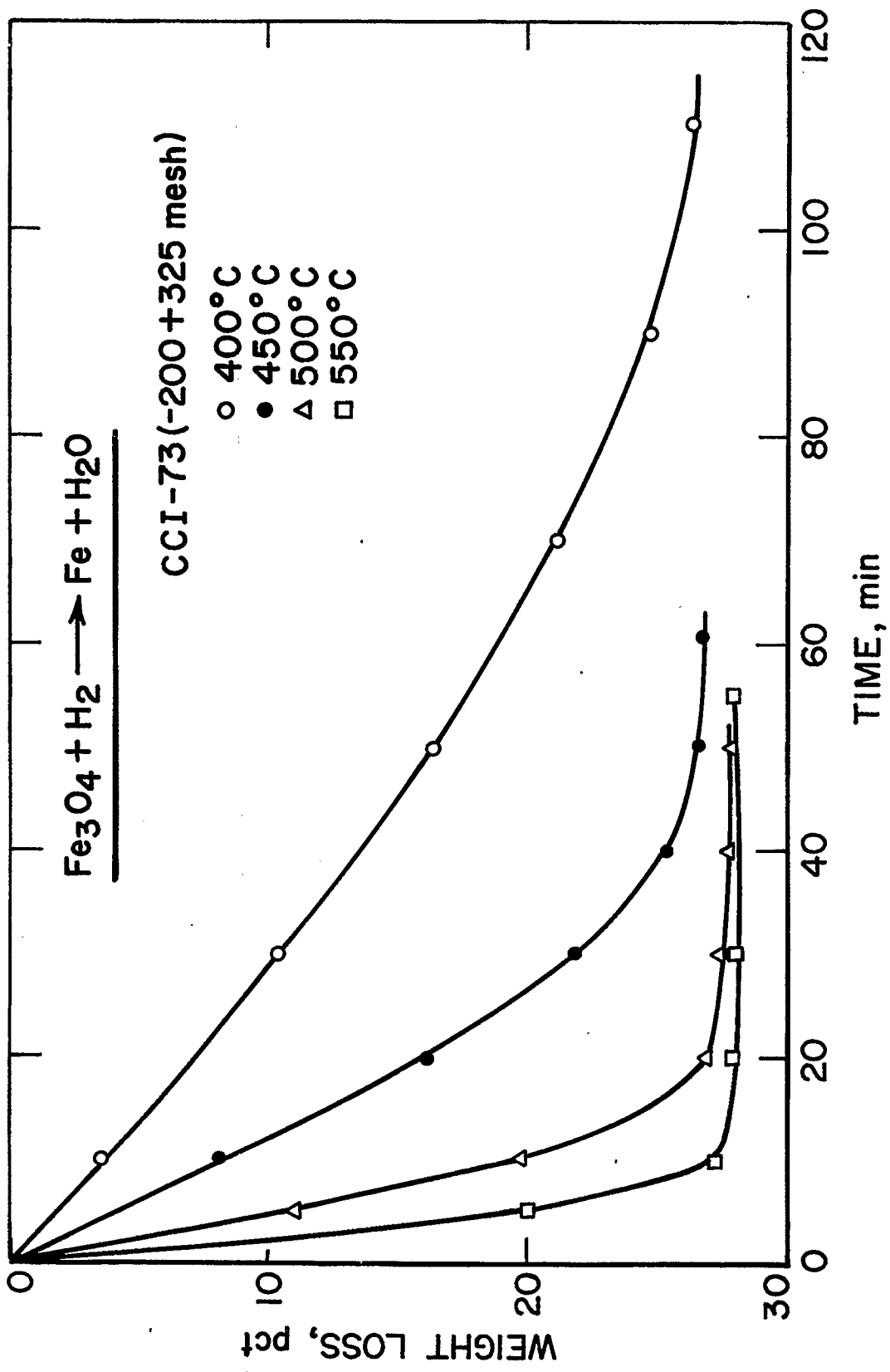


Figure 17 - Reduction of 200/325 mesh fused iron catalyst as a function of temperature.

5-12-80 L-17658

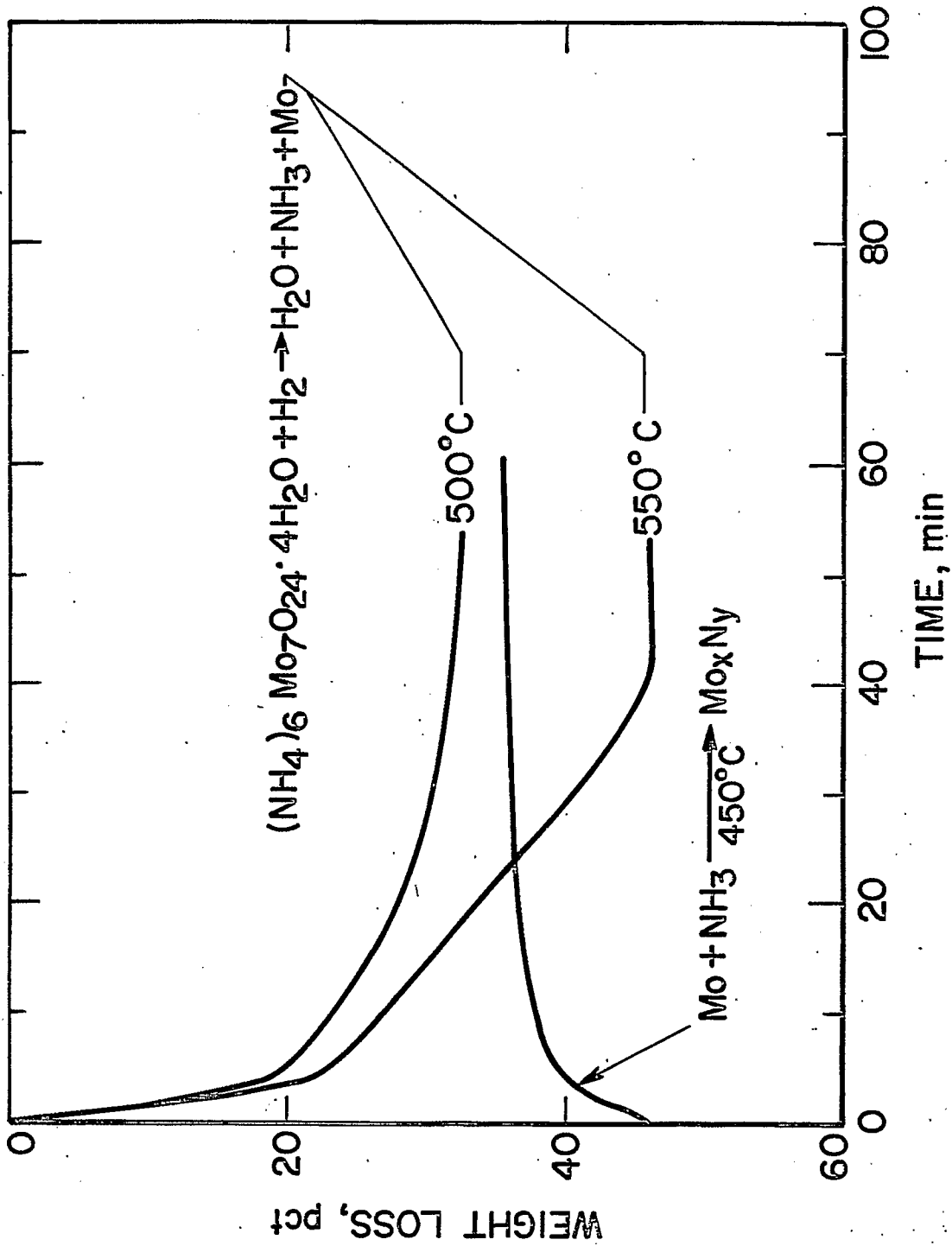


Figure 18- Reduction of Ammonium Molybdate by H₂.

5-12-80 L-17663

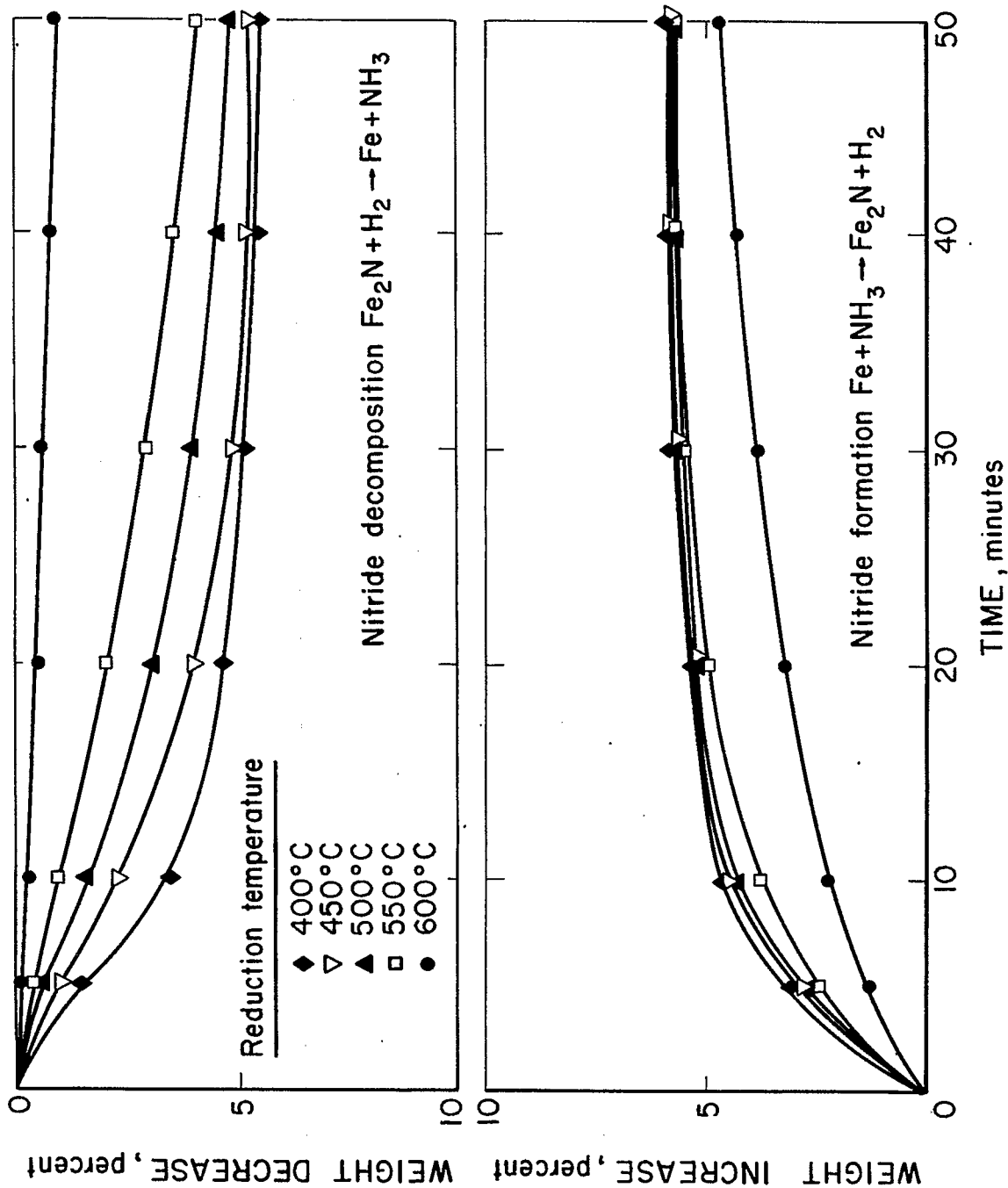


Figure 19 - Rates of nitride formation and nitride decomposition .

12-31-79 L-17263

for reduction to occur. Since iron molybdate is more stable than aluminum molybdate, another interaction that might occur is that of unreduced iron oxide with molybdenum oxide. Neither compound could be identified using x-ray diffraction.

In the case of the Mo-promoted catalysts, since the reduction temperature selected, 500°C, was considerably higher than that required for reduction of Fe_3O_4 , a study was carried out to determine the effect of reduction temperature on the rate of nitridding and also on the stability of the nitride in H_2 . The effect of reduction temperature on the rate of nitride formation is shown in the bottom graph of Figure 19. These data show clearly that catalysts reduced at higher temperatures nitrided more slowly. In the top graph the reaction of the nitride with H_2 at 175°C is shown to proceed more slowly as the catalyst reduction temperature was increased. Reduction at 600°C resulted in a nitride far less reactive towards hydrogen than did reduction at 400°C. Since increased nitride stability was a desirable objective, it appeared at first glance that varying reduction temperature was a useful way to modify nitride stability.

As shown in Table 2, subsequent x-ray diffraction measurements indicated, however, that the T.G.A. data did not reflect a difference in the inherent stability of the nitride but were a result of differences in the metallic iron surface area of the reduced catalyst, i.e., the lower reactivity observed for catalysts reduced at higher temperatures was the result of a significant difference in the amount of iron and iron nitride exposed to NH_3 and H_2 , respectively.

TABLE 2
CRYSTALLITE SIZE OF REDUCED FUSED IRON CATALYSTS

<u>Reduction Temperature</u>	<u>Crystallite Size, Å</u>
400°C	370
450°C	450
500°C	500
550°C	600

All catalysts were reduced for one hour.

These values represent relative values and should be used only for making comparisons of crystallite size. Since the primary objective of the nitrated iron catalyst study was to prepare a more stable nitride, presumably by incorporation of molybdenum into the catalyst, an attempt was made to develop a T.G.A. technique that would provide a measure of nitride stability.

Initially it had to be determined if the nitride instability was due to thermal decomposition of the iron nitride, resulting in a metallic iron species that was immediately converted to the carbonitride or carbide in the synthesis gas atmosphere. The decomposition of iron nitride in a helium atmosphere is shown in Figure 20. Both the reference catalyst and the Mo-promoted catalyst were reduced at 550°C and nitrated at 450°C. The difference in the rates of decomposition was within experimental error. Since no decomposition was observed at temperatures lower than 300°C, it was felt that thermal decomposition did not contribute significantly to carbonitride formation when studying synthesis gas conversion in the 220°C-270°C temperature range.

While definitive evidence is not available on the mechanism for conversion of iron nitride to the corresponding carbonitride or carbide, one possible mechanism is a two-step reaction:

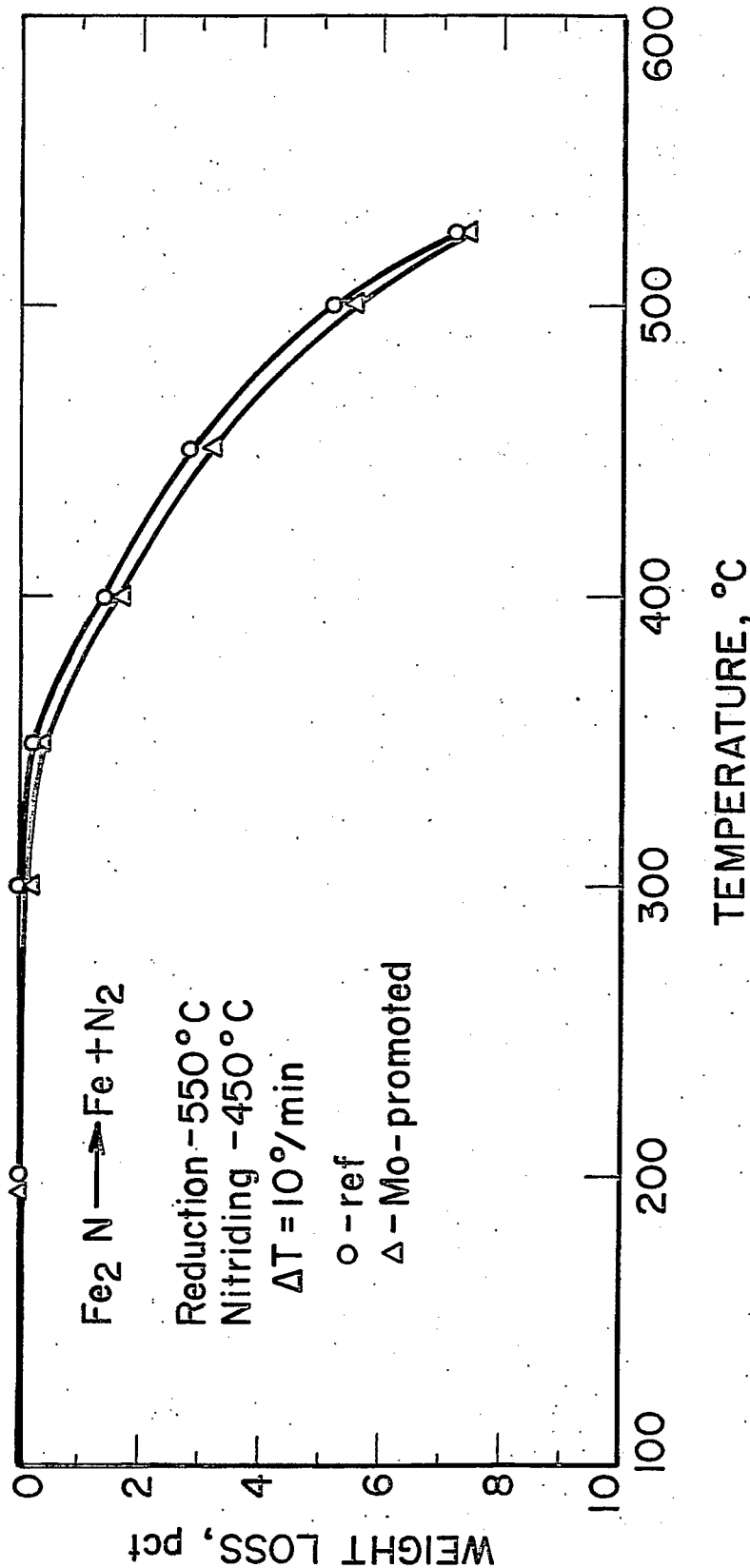
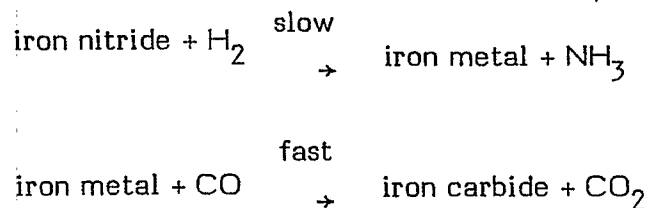


Figure 20 - Decomposition of Fe_2N in He.

5-12-80 L-17653



While it would have been most appropriate to determine the stability in a synthesis gas atmosphere, conversion of the nitride to a carbonitride or to the carbide resulted in an insignificant weight loss. The difficulty of measuring this weight loss accurately was compounded by the fact that three additional weight changes occurred. These weight changes resulted from the following:

1. Buoyancy effect resulting from differences in the densities of helium and synthesis gas.
2. Accumulation of carbonaceous deposits on the catalyst surface.
3. Oxidation of the surface by water vapor or carbon dioxide.

For these reasons no definitive T.G.A. data on nitride stability in a synthesis gas atmosphere were obtained.

If, in fact, reaction of the nitride with H_2 was the rate-determining step, then nitride stability in a pure H_2 atmosphere might be a useful technique for predicting catalyst stability under synthesis gas conversion conditions. Figure 21 shows the results obtained for the reaction of the unpromoted nitrided catalyst and the Mo-promoted nitrided catalyst with H_2 at 175°C . In spite of the fact that Mo-promoted nitrided catalysts showed greater activity in the microreactor tests, these T.G.A. data indicated that it was less stable, i.e., more reactive, in a H_2 atmosphere. It is important to keep in mind that the T.G.A. measurements do not

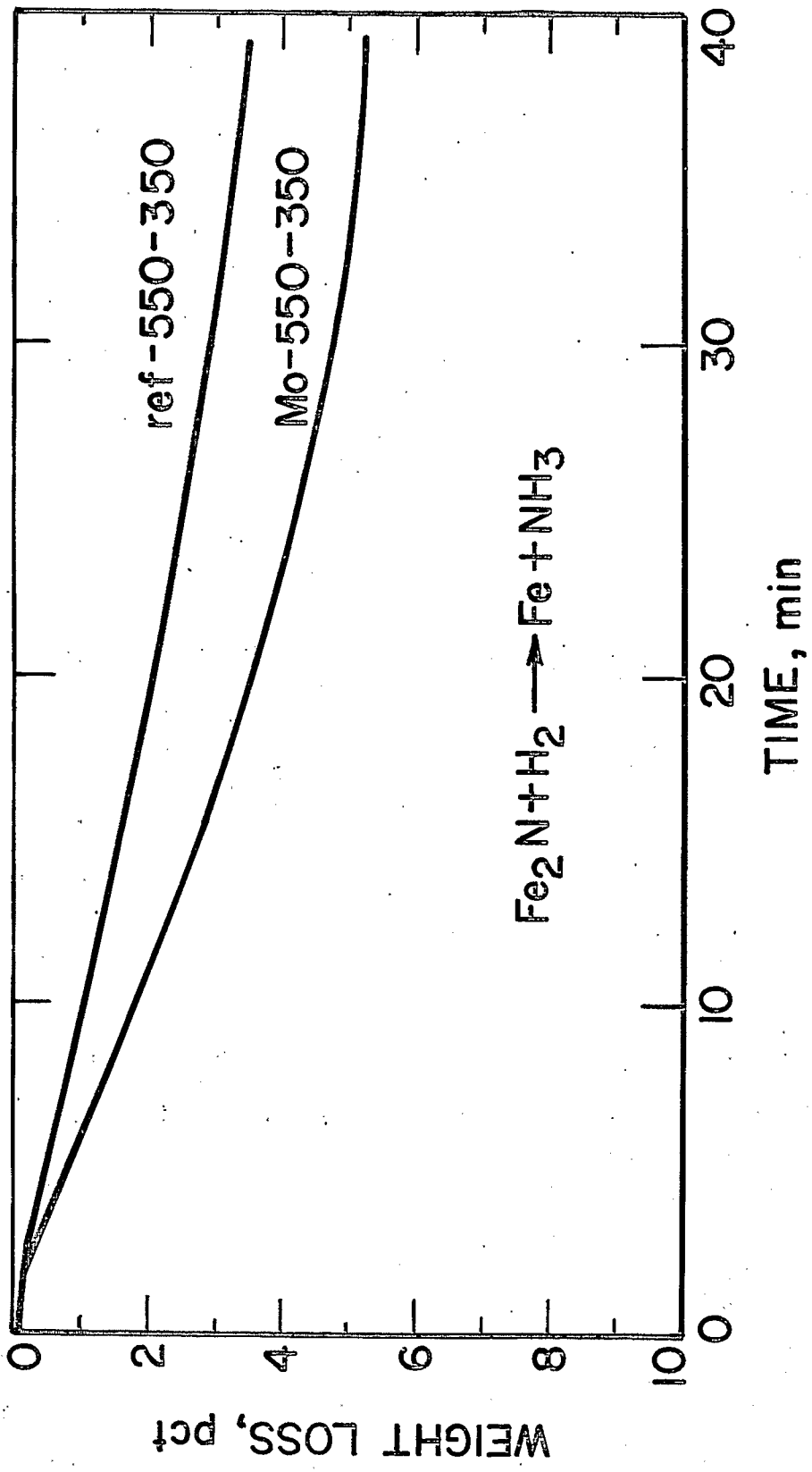


Figure 21- Reaction of iron nitrides with H₂ at 175°C.

5-12-80 L-17654

necessarily reflect changes in the inherent stability of these materials. If the Mo/N stoichiometric ratio is less than the Fe/N stoichiometric ratio, this could result in greater exposure of the nitrogen atoms, resulting in a more rapid weight loss. If unreduced MoO_3 minimized sintering of the iron crystallites (in a manner similar to that of CaO and Al_2O_3), then the resulting greater surface area of the Mo-promoted catalyst would result in increased reactivity towards hydrogen. The fact that reaction occurred so readily at a temperature of 175°C , significantly lower than that required for synthesis gas conversion, indicated that nitride stability as determined in a H_2 atmosphere might be too simplistic a measure of stability in a synthesis gas atmosphere. Preferential chemisorption of CO on the iron surface at least partially accounted for the observation that nitrides were much more stable in synthesis gas atmospheres, as evidenced by previous Bureau of Mines (B.O.M.) synthesis studies that extended for hundreds of hours. The fact that in the B.O.M. studies the nitrides were only slowly converted to carbonitrides at temperatures as high as 250°C and pressures of 21.4 atm ($\text{H}_2/\text{CO} = 1$) is in sharp contrast to our observation that nitrides were quite unstable in a pure H_2 atmosphere. Our explanation that involves preferential chemisorption of CO is also consistent with the strong positive dependence of the rate expression on the H_2 partial pressure.

The dependence of the conversion of synthesis gas on the hydrogen partial pressure has been determined by a number of workers. Dry (8) found the following expression when working with a fused iron catalyst:

$$\text{rate} = kP_{\text{H}_2}$$

Vannice(9) found that the rate of methane formation, using a 15% Fe/Al₂O₃ catalyst, could be described by the following expression:

$$\text{Rate} = N_{\text{C}_{\text{H}_2}} = A e^{E_m/RT} P_{\text{H}_2}^x P_{\text{CO}}^y$$

where $x = 1.14 \pm 0.10$

$y = 0.05 \pm 0.07$

Microreactor Testing

Single Stage

The microreactor testing described in this report is concerned exclusively with establishing the effectiveness of molybdenum as a promoter for fused iron catalysts. The results are shown in Table 3.

The pertinent conversion data can be summarized as shown in Table 4.

TABLE 4
CONVERSION DATA SUMMARY - Mo PROMOTED VS. UNPROMOTED CATALYSTS

	<u>Reaction Temperature</u>	<u>Average Percent Conversion</u>
Unpromoted, reduced @ 450°C	270	15 (#2, 13)
	250	10 (#10)
Mo-promoted, reduced @ 450°C	270	23 (#3, 14)
Mo-promoted, reduced @ 550°C	270	40 (#4, 6, 12)
	250	25 (#11, 15)
Unpromoted, reduced @ 550°C	270	9 (#94)

(#-run number)

TABLE 3
SINGLE-STAGE MICROREACTOR TEST DATA

Run #	2	3	4	6	7	9	10	11	12	13	14	15	16	94
Catalyst	---	Mo	Mo	Mo	Mo	---	---	Mo	Mo	---	Mo	Mo	---	---
Space Velocity $\times 10^{-3}$	5	5	5	5	15	5	2.5	5	5	5	5	5	5	5
Reduction Temp. $^{\circ}\text{C}$	450	450	550	550	550	450	450	550	550	450	450	550	450	550
Reaction Temp. $^{\circ}\text{C}$	270	270	270	270	270	270	250	250	270	270	270	250	250	270
Carbon Balance	0.80	0.79	0.86	0.83	0.84	0.94	0.95	0.81	0.93	0.91	0.80	0.87	0.98	0.82
Conversion %	18	25	39	36	19	6	21	26	45	12	22	25	10	9
Wt.% CH_4	15	21	10	19	20	12	14	15	19	15	17	15	17	14
Wt.% C_2H_4	11	12	3	5	7	11	9	6	5	8	9	7	11	12
wt.% C_2H_6	4	7	9	8	8	--	5	6	8	3	5	6	4	6
wt.% C_3H_6	16	22	15	15	17	8	14	12	15	12	13	14	17	13
wt.% C_3H_8	4	5	5	4	4	--	5	4	3	8	3	3	--	5
Wt.% C_4H_8	--	--	--	--	--	--	--	--	--	--	--	--	--	--

TABLE 3, Cont.

Run #	2	3	4	6	7	9	10	11	12	13	14	15	16	94
Catalyst	---	Mo	Mo	Mo	Mo	---	---	Mo	Mo	---	Mo	Mo	---	---
wt. % C ₄ H ₁₀	--	4	3	2	--	--	--	--	3	--	--	--	--	--
wt. % C ₅₊	49	29	44	47	44	69	52	58	48	54	53	55	50	48

Analysis, C₅₊

Simulated

Dist.	93	96	82	84	96	93	95	83	82	--	96	96	68
-------	----	----	----	----	----	----	----	----	----	----	----	----	----

Infrared,

CO ₂ R	0.8	0.9	0.6	0.8	0.7	1.1	1.1	0.8	1.1	1.2	0.7	0.6
CO	1.1	1.0	1.0	.9	.8	2.4	2.3	1.8	1.7	2.5	2.0	1.8
CO ₂ H	0.8	0.8	0.8	0.8	1.1	0.7	0.7	0.5	0.6	0.6	0.5	0.5
C=C	9.4	12	9.0	9.3	11.6	9.4	8.1	8.2	9.2	8.5	9.9	8.6
C=C(2)	1.3	1.8	3.9	3.3	2.6	2.0	1.7	2.0	2.8	2.2	1.4	1.5
C=C(Br)	0.7	0.7	0.7	0.6	0.6	0.8	0.9	0.7	0.5	1.2	0.9	0.8
OH	6.6	5.8	2.6	3.4	5.1	9.5	10.2	7.2	4.3	11.3	9.5	10.1
Br #	75	97	91	88	99	82	72	73	83	79	81	72

Analysis, Aqueous Product

%(w/w) H ₂ O				73		70					60		66
----------------------------	--	--	--	----	--	----	--	--	--	--	----	--	----

It is apparent from Table 4 that the Mo-promoted catalyst was considerably more active than the unpromoted catalyst. Reduction of the Mo-promoted catalyst at higher temperatures (550°C) resulted in the most active catalyst, in spite of the fact that significant sintering of the iron crystallites was found when reduction was carried out at that temperature. This is reflected in the low conversion found for the unpromoted catalyst reduced at 550°C .

The mechanism for the promoting action of Mo will be speculated on briefly. It is possible that in fact a Fe-Mo nitride catalyst was formed, which was the original intent of this effort. The higher activity observed for catalysts reduced at 550°C may have been due to the fact that this temperature, as suggested by the T.G.A. studies, was required for reduction of ammonium molybdate to Mo metal.

The second possible mechanism is the formation of a Mo-containing species on the catalyst surface, which causes significant rate enhancement. In this regard it first should be pointed out that a number of investigators have established; using selective chemisorption of CO and CO_2 as well as N_2 physical adsorption, that a reduced magnetite surface is made up to a large degree of the various oxides used as promoters, even though these promoters make up only a few percent of the bulk composition of the catalyst. Possibly the ammonium molybdate is converted to MoO_3 , which at 550°C will react with Al_2O_3 (10) as shown in Figure 22 to yield the Mo-containing species shown. These reduced molybdenum catalysts are known to have good hydrogenation activity.

As far as selectivity is concerned no significant difference was found in the amount of C_{5+} product or in the amount of C_{5+} product boiling less than 400°F , as

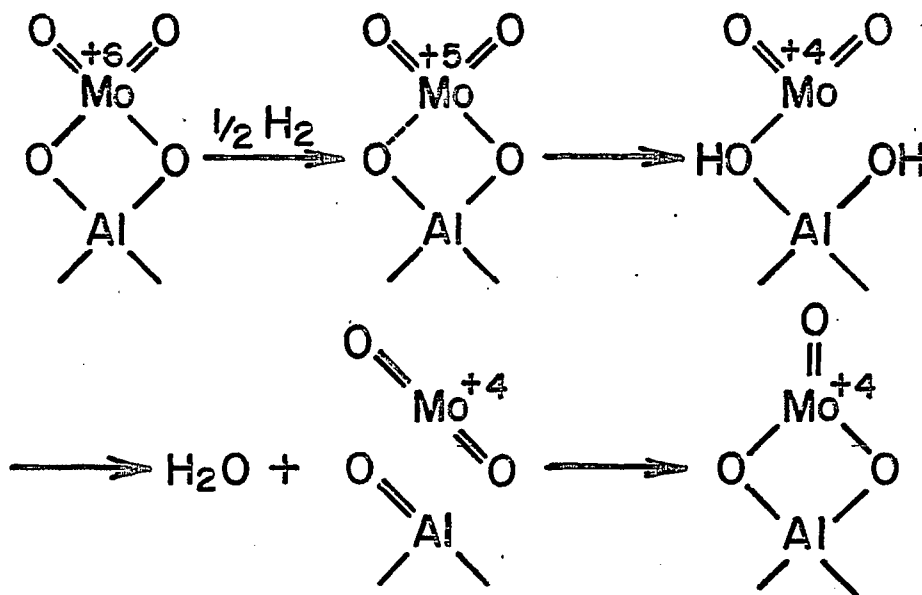
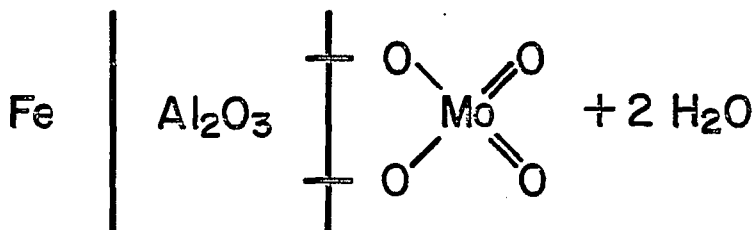
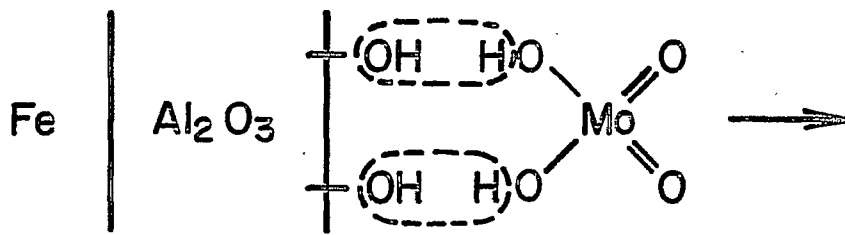


Figure 22 - Reaction sequence involving interaction of MoO_3 with Al_2O_3 .

5-14-8 L-17662

determined using simulated distillation. There did appear, however, to be a significant decrease in the oxygenate content of the C₅₊ product using infrared analysis.

The analysis of the aqueous layer for oxygenates (Table 5) was consistent with results obtained in the earlier Bureau of Mines studies. As indicated in Table 3, the oxygenate content of the aqueous layer ranged from 27 to 40 wt.%. The bulk of these oxygenates were normal alcohols, although methanol was found in only small amounts.

TABLE 5
G. C. ANALYSIS (AQUEOUS LAYER)

METHANOL	1.8 wt.%
ETHANOL	59.4
ACETONE	4.6
2-PROPANOL	1.4
N-PROPANOL	17.2
METHYL ETHYL KETONE	2.2
2-BUTANOL	1.1
2-METHYL-1-PROPANOL	0.4
N-BUTANOL	6.4
2-PENTANOL	0.4
1-PENTANOL	5.2

On-Line Microreactor

Some of the problems associated with the study of catalysts for the Fischer-Tropsch reaction included a lack of continuous analysis over a wide range of carbon numbers and a less than accurate analysis of the C_4 - C_8 fraction produced in the reaction. The difficulty encountered in accurately determining the C_4 - C_8 fraction lies in the fact that these hydrocarbons distribute themselves in both the gas and liquid phases. Hence, a measure of these carbon numbers in only the gas phase represents an incomplete analysis. Additionally, the volatility of this carbon fraction gives rise to partial loss from the liquid phase, which again results in an incomplete analysis of this phase.

It was felt that an on-line gas chromatographic analysis could provide a continuous as well as complete analysis of the Fischer-Tropsch product. A major problem associated with the implementation of this technique, however, was caused by the fact that Fischer-Tropsch reactions are generally conducted at 100-300 psig. Introduction of a sample into the carrier gas stream at this pressure caused considerable peak spreading. As a result, peak resolution is far poorer than that obtained with a sample introduced at atmospheric pressure. An additional problem involved keeping the entire Fischer-Tropsch product in the gaseous state from the reactor to the sampling valves.

The gas chromatograph procedure was able to distinguish the seven compounds shown in Table 6 using the thermal conductivity detector (Carbosieve column), and C_1 - C_{20} hydrocarbons using the flame ionization detector (SP2100 column). The retention times of the various compounds are listed in Tables 6 and 7. Hydrocarbons as high as C_{24} could also be detected, but due to their low weight

fraction relative to all hydrocarbons, a determination of their percent composition was less accurate than other hydrocarbons. In general, the C_1 - C_{20} hydrocarbons represented >98% of all hydrocarbons, and therefore the decision was made to end the analysis at C_{20} . A typical chromatogram is illustrated in Figure 23.

The weight fraction of a specific carbon number, W_n , obtained from the gas chromatograph analysis was used to generate an Anderson-Schulz-Flory plot. From such a plot it was possible to determine the polymerization probability, p , either from the intercept or the slope. Figure 24 shows the Anderson-Schulz-Flory plot generated from the weight fraction data. The data illustrated in Figure 24 were taken from a catalyst run that had been on-stream only 310 min. In the past, this detailed information would have been very difficult to obtain after so short a time.

Another advantage of this method of analysis was the opportunity to examine the change in catalyst selectivity over a period of time. For example, Tables 8 and 9 show the change in selectivity with time. It is apparent that the catalyst had not yet achieved a steady state composition in view of the small but definite trend toward greater light hydrocarbon (C_1 - C_4) formation.

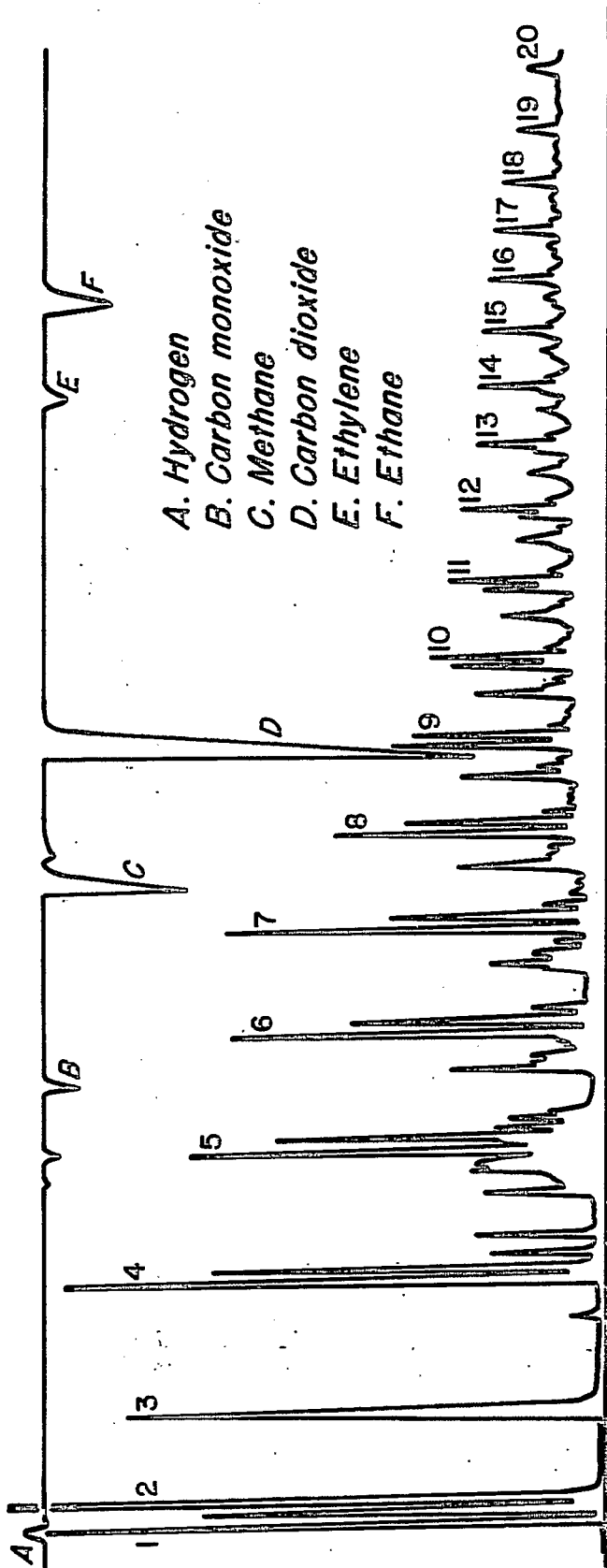


Figure 23 - Gas chromatogram of Fischer - Tropsch Product . Peaks numbered 1-20 represent C₁-C₂₀ hydrocarbons as detected by FID. Peaks labeled A-F were detected on the TCD.

L-81288

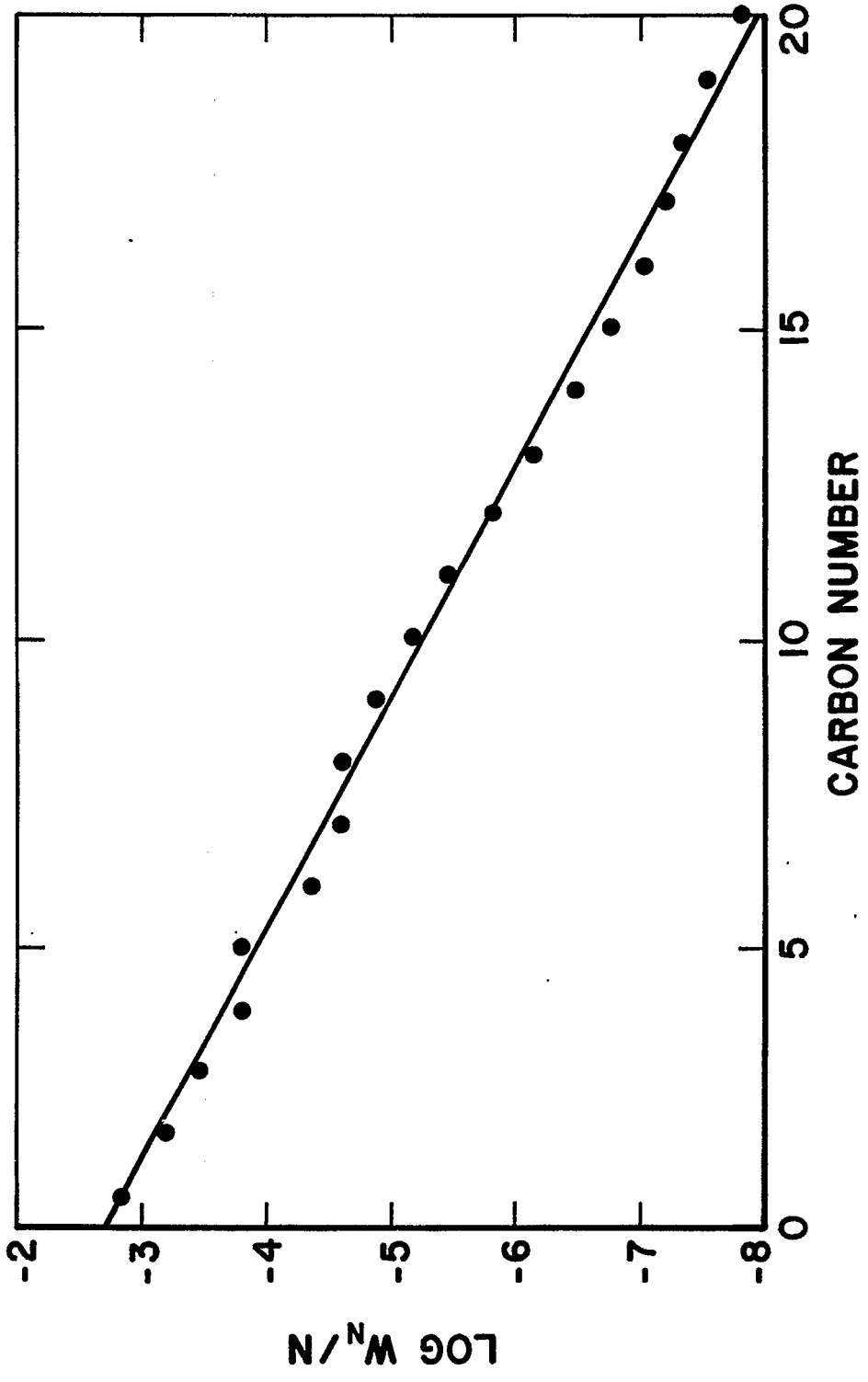


Figure 24-Anderson - Schulz - Flory Plot of C-73-2 Fused Iron Catalyst (T = 573°K, H₂/CO = 3).

L-81289

TABLE 6
RETENTION TIMES FOR COMPOUNDS DETECTED BY TCD

Compound	Time (min)
H ₂	1.63
CO	15.65
CH ₄	22.21
H ₂ O	23.26
CO ₂	26.58
C ₂ H ₄	37.95
C ₂ H ₆	41.06

TABLE 7
RETENTION TIMES FOR COMPOUNDS DETECTED BY FID

Compound	Time Frame(min)
CH ₄	1.62
C ₂ H ₄	1.97
C ₂ H ₆	2.37
C ₃ H ₆	5.06
C ₃ H ₈	5.31
C ₄ *	8.31-11.01
C ₅ *	12.05-15.00
C ₆ *	16.41-18.46
C ₇ *	18.79-21.80
C ₈ *	22.55-25.60
C ₉ *	26.03-28.12
C ₁₀ *	28.73-30.65
C ₁₁ *	31.25-33.02
C ₁₂ *	33.61-34.88
C ₁₃ *	35.25-36.93
C ₁₄ *	37.79-38.85
C ₁₅ *	39.50-40.64
C ₁₆ *	41.22-42.84
C ₁₇ *	43.13-43.92
C ₁₈ *	44.38-45.49
C ₁₉ *	45.96-47.25
C ₂₀ *	47.74-49.27

*Retention times for C_n(n=4-20) fractions are given for all C_n compounds that are eluted over the time frame shown.

TABLE 8
CHANGE IN AVERAGE DEGREE OF POLYMERIZATION WITH TIME*

Time(min)	P	D
310	0.769	4.33
1354	0.768	4.31
1828	0.762	4.21
2510	0.752	4.04

*CCI catalyst, 300°C, 300 psig, 3/1 syn gas, GHSV: 3600 (v/w)h⁻¹

TABLE 9
CHANGE IN HYDROCARBON DISTRIBUTION WITH TIME*

Time(min)	C ₁ -C ₄ (calcd)**	Weight Percent C ₅ -C ₁₁ (calcd)**	C ₉ -C ₂₀ (calcd)**
310	32.13(32.69)	51.50(47.59)	34.19(31.92)
1354	36.71(32.93)	47.45(47.60)	29.34(31.68)
1828	36.16(34.04)	48.97(47.62)	31.30(30.63)
2510	40.78(42.39)	46.31(47.49)	26.01(28.55)

*CCI catalyst, 300°C, 300 psig, 3/1 syn gas, GHSV: 3600 (v/w)h⁻¹

**Values in parentheses represent theoretically calculated values as obtained from experimentally determined p values.

FUTURE STUDIES

It has been established that a Mo-promoted nitrided fused iron catalyst is significantly more active than the unpromoted catalyst at 270°C. Additional microreactor runs will be required to determine if Mo-promoted catalysts are more active and stable at reaction conditions that more closely simulate the conditions likely to be found in commercial-size reactors, namely, 230°C-250°C.

Additional studies will be carried out to provide a better understanding of the mechanism of catalyst promotion--a catalyst species containing Mo as Mo₂N, Mo₂C, or (Fe_xMo_y)N, or, on the other hand, a species such as MoO₃·Al₂O₃, which is known to be a good hydrogenation catalyst. Preliminary ESCA and SIMS data indicate that the surface of both reduced and unreduced Mo-promoted catalysts consists largely of potassium and molybdenum. The concentration of alumina on the surface is probably too low to determine if it is interacting with MoO₃. The use of an in situ reduction attachment on the SIMS unit may permit the identification of the oxidation state of the reduced promoted catalysts.

Microreactor, x-ray, and T.G.A. studies will continue with samples prepared at Los Alamos National Laboratory. These samples include the following:

1. (Fe, Mo₁₃)N
2. Mo₂N
3. Fe₄N
4. MoCo_{.48}
5. NbN
6. Nb_{.984}N_{.807}C_{.163}

7. NbN_{.489}C_{.495}

Catalyst samples 2, 3, and 4 represent the end members of the Fe, N, Mo, C system (the behavior of Fe₂C has already been established). Sample 1 represents the composition indicating the solubility limit of Mo in iron nitride. Since there is some indication that niobium has activity for synthesis gas conversion, samples 5-7 will also be investigated.

BIBLIOGRAPHY

1. Storch, H. H., Anderson, R. B., Hofer, L. J. E., Hawk, C. O., Anderson, H. C., and N. Golumbic, Synthetic Liquid Fuels from Hydrogenation of Carbon Monoxide, Technical Paper 709, U.S. Government Printing Office, 1948.
2. Shultz, J. F., Hofer, L. J. E., Stein, K. C., and R. B. Anderson, Carbides, Nitrides, and Carbonitrides of Iron as Catalysts in the Fischer-Tropsch Synthesis, Bulletin 612, U.S. Government Printing Office, 1963.
3. Anderson, R. B., Karn, F. S., and J. F. Shultz, Kinetics of the Fischer-Tropsch Synthesis on Iron Catalysts, Bulletin 614, U.S. Government Printing Office, 1964.
4. Meisel, S. L., McCullough, J. P., Lechthaler, C. H., and P. B. Weisz, Chem. Tech, 6, 86 (1976).
5. Goldschmidt, H. J., Interstitial Alloys, Plenum Press, New York, 1967.
6. Burton, James, J., and Robert L. Garten, ed., Advanced Materials in Catalysis, Academic Press, 1977.
7. Dry, M. E., Shingles, T., Boshoff, L. J., and G. J. Oosthuizen, J. Catal., 15, 190 (1969).
8. Dry, M. E., Shingles, T., and L. J. Boshoff, J. Catal., 25, 99 (1972).
9. Vannice, M. A., Catal. Rev.-Sci. Eng., 14(2), 153 (1976).
10. Lombardo, E. A. Houalla, M., and W. Keith Hall, J. Catal., 51, 256 (1978).

APPENDIX A. PREPARATION AND COMPOSITION OF CATALYSTS

The catalysts used in this study were all fused iron oxide catalysts, as received or impregnated with various promoters. The reference, or standard catalyst, was CCI-73, a commercially available ammonia synthesis catalyst and similar to the catalyst used in the entrained-bed reactors at SASOL. As shown in Table 7, it contained small amounts of the "structural promoters" Al_2O_3 , MgO , and CaO as well as the "chemical promoter" K_2O . In addition, five other catalysts were studied.

TABLE 10
CATALYST COMPOSITION AND METHOD OF PREPARATION
(-200 + 325 mesh)

<u>Catalyst</u>	<u>% Fe</u>	<u>CaO</u>	<u>MgO</u>	<u>Al_2O_3</u>	<u>SiO_2</u>	<u>K_2O</u>	<u>CuO</u>	<u>MoO_3</u>
1-reference	67.1	1.82	0.17	3.02	0.21	0.60	0.01	---
2	6.56	"	"	"	"	5.20	0.01	---
	Dipped in a saturated solution of K_2CO_3 for 10 minutes, suction-filtered, and oven-dried.							
3	64.7	"	"	"	"	0.50	1.60	--
	Dipped in a copper nitrate solution, 6% Cu by weight, for 20 minutes, suction-filtered, and oven-dried.							
4	64.6	"	"	"	"	0.50	1.80	--
	Dipped in a copper nitrate solution, 6% Cu by weight, for 60 minutes, suction-filtered, and oven-dried.							
5	65.0	"	"	"	"	1.10	0.02	--
	Dipped in a solution of K_2CO_3 , 12% K by weight, for 10 minutes, suction-filtered, and oven-dried.							
6	65.0	"	"	"	"	0.50	0.01	--
	Dipped in a solution of ammonium molybdate, 40 g. $(\text{NH}_4)_6\text{Mo}_7\text{O}_{24} \cdot 4\text{H}_2\text{O}/100 \text{ ml. H}_2\text{O}$, for 10 minutes, suction-filtered, and oven-dried.							

TABLE 11
 CATALYST COMPOSITION AND METHOD OF PREPARATION
 (-3½ + 7 mesh)

<u>Catalyst</u>	<u>% Fe</u>	<u>CaO</u>	<u>MgO</u>	<u>Al₂O₃</u>	<u>SiO₂</u>	<u>K₂O</u>	<u>CuO</u>
7	67.1	1.82	0.17	3.02	0.21	0.60	0.01
8	65.0	"	"	"	"	1.00	0.01
	Dipped in a saturated solution of K ₂ CO ₃ for 60 minutes, drained of liquid, and oven-dried.						
9	66.1	"	"	"	"	0.60	0.10

Dipped in a copper nitrate solution, 6% Cu by weight for 60 minutes, drained of liquid, and oven-dried.

Ditto marks indicate the percentage of that constituent, while not actually measured, was nominally the same as that in the unpromoted catalyst.

APPENDIX B. THERMOGRAVIMETRIC ANALYSIS PROCEDURE

A Perkin-Elmer TGS-2 analyzer system was used to study the rates of reduction, carbiding, and nitriding of the catalysts, and the rates of decomposition of the carbides and nitrides.

The principle unit of the system was the recording microbalance (Figure 25). The balance was used to record the weight changes of samples subjected to a controlled environment. Quartz stirrups were suspended from the balance to contain the samples and to tare the balance. The weighing mechanism was purged continuously with 10 mL/min helium to insure that none of the reactant gases, such as hydrogen, carbon monoxide, and helium, nor any product gas, such as water vapor, could enter the balance mechanism compartment and damage the delicate parts. The temperature controller unit allowed the operator to program and monitor all aspects of temperature control, such as the rates of heating and cooling. A chromel-alumel thermocouple was used for temperature measurement, and the results were recorded on an X-Y recorder.

The system had a sample weight limit of 100 mg and a temperature range of 27° to 1000°K. The procedure for operating the TGS involved placing the sample on the balance, controlling its environment, and recording its weight change. Initially, it was necessary to zero both the X-Y recorder and the balance. About 10 mg of the (200/325) catalyst was placed in the quartz bucket, and the furnace raised to enclose the sample. The sample was then weighed to six significant figures in a helium atmosphere (200 mL/min). To magnify the weight change as observed on the recorder, the balance was set to suppress electronically a given amount of the sample weight; the recorder then indicated the degree of weight change on a much larger scale. Typically 50% weight suppression was used.

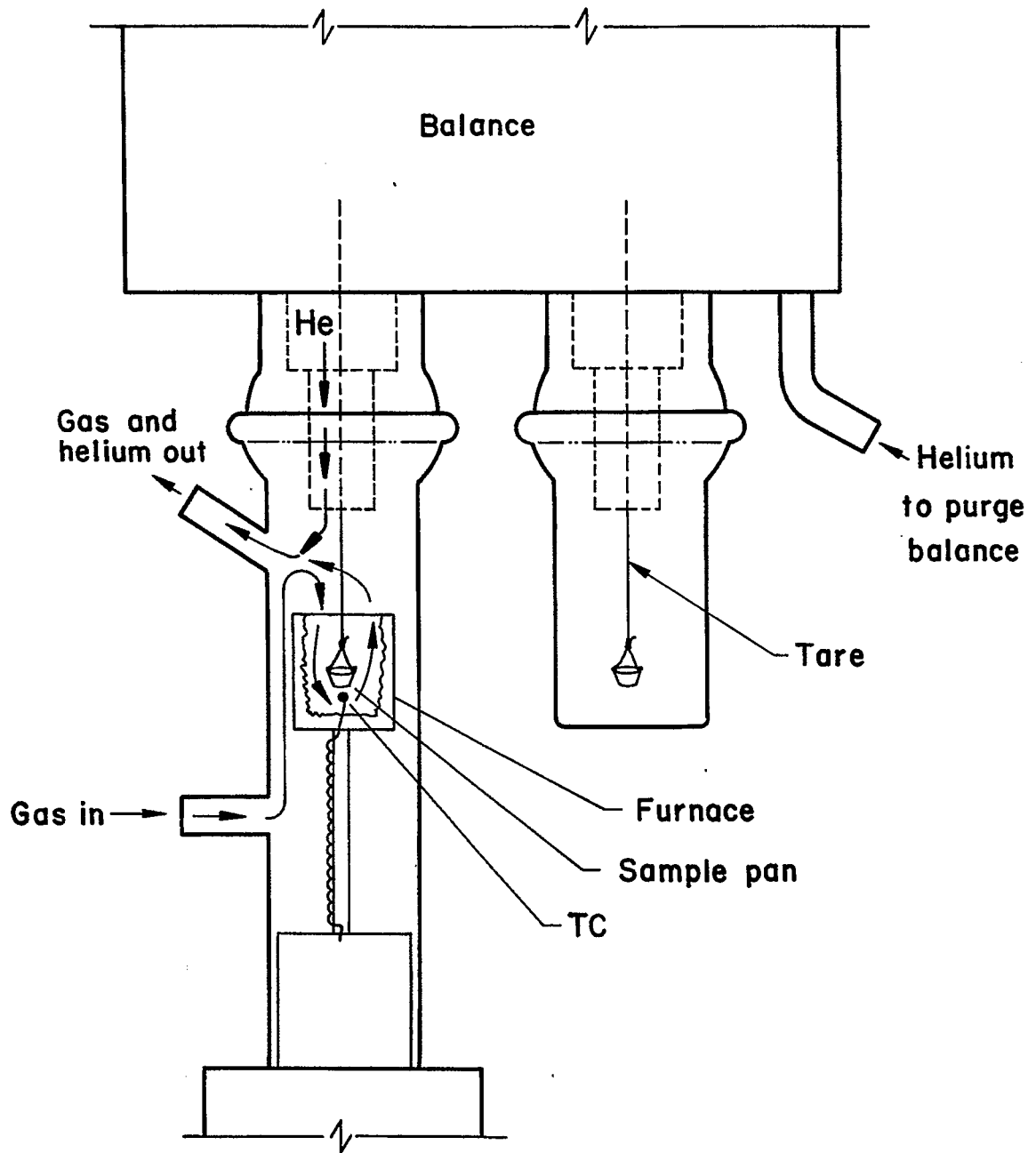


Figure 25 - Thermogravimetric balance

7-24-79 L-16866

A three-way valve permitted switching gases without admitting air to the sample environment. The minimum and maximum furnace temperatures were set at 50°C and 600°C, respectively.

In order to carry out an efficient microreactor testing study, it was necessary to determine the most effective temperature to use for catalyst reduction, carbiding, and nitriding. For this reason it was necessary to study the rate of reaction as a function of temperature, as indicated in Figure 25. It will be noted that the fused iron catalyst (magnetite) is not reduced in a hydrogen atmosphere until the temperature reached about 270°C. (The rate of temperature increase was 0.1°C/min.) Figure 26 shows the reaction proceeded rapidly to completion at temperatures in excess of 350°C. After reduction, the sample was purged from the unit with helium, and the temperature was reduced to 100°C. Flowing ammonia was then used as the gaseous environment, and the temperature was increased at the rate of 1°C/min. The rate of nitriding was insignificant at temperatures less than 200°C. After the sample had been completely nitrified at a temperature of 350°C, the temperature was decreased to 100°C, and the ammonia was expelled from the unit using a helium purge gas. Then the sample temperature was increased at a rate of 1°C/min in a flowing hydrogen atmosphere. As indicated, nitride decomposition occurred readily at a temperature of about 175°C. This procedure was also used to determine the temperatures required for carbide formation and decomposition.

Once the temperature required for effecting a given reaction had been determined using the just-described procedure, it was often desirable to make a comparison of the reactivities of various catalytic materials (oxides, nitrides, reduced catalysts, and carbides) with reactive gases. Rather than carry out

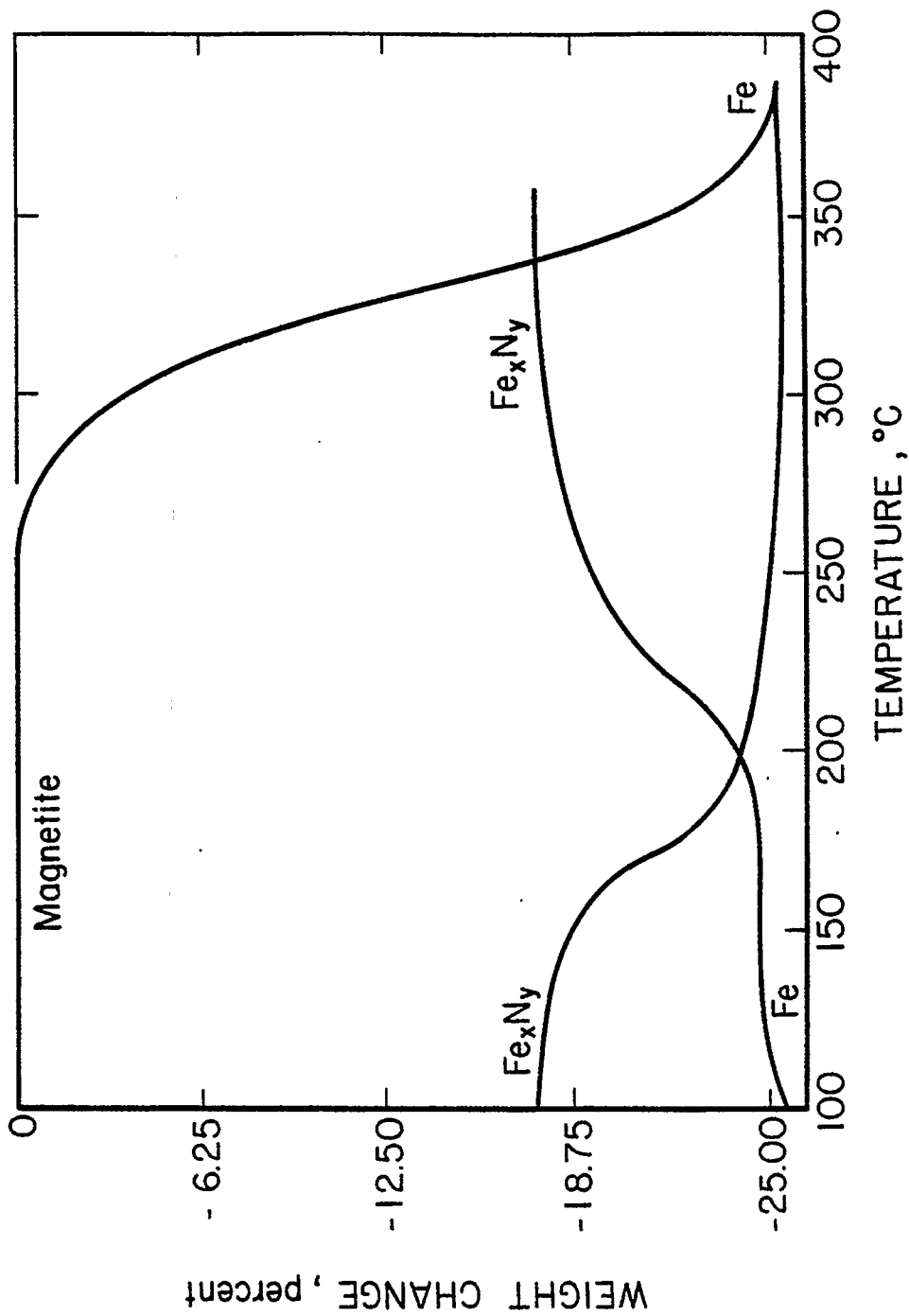


Figure 26- $\text{Fe}_3\text{O}_4 \rightarrow \text{Fe} \rightarrow \text{Fe}_x\text{N}_y$ transformations

5-12-80 L-17656

temperature scans as described earlier, a more sensitive measure of reactivity was to measure the relevant weight change at a given temperature. Temperatures were chosen so that reactivities could be measured in a reasonable period of time; however, care had to be taken to insure the temperature was not so high that only bulk diffusion of the gas to the catalyst sample was being measured. Bulk diffusion could be eliminated as the rate-determining step by working only in a temperature range in which the reactivity (weight change/unit time) was independent of the catalyst weight and reactive gas flow rate.

APPENDIX C. MICROREACTOR TESTING PROCEDURE

Two different microreactor unit configurations were used to determine the reactivity of the catalysts for synthesis gas conversion. The first configuration provided for on-line analysis of the product stream, and details are shown in Figures 27- 29. The second configuration differed from the first in that, instead of on-line analysis, an ice trap immediately downstream of the reactor was used to condense the aqueous product containing light alcohols as well as C_{5+} hydrocarbons. (The gas chromatograph was removed from the unit.) The gaseous product was collected in a sample bottle.

Regardless of configuration, the microreactor itself was a continuous-flow fixed-bed reactor with the dimensions of 16" length, 1/4" i.d., 3/8" o.d., constructed from 316 stainless steel. Initially, the reactor was placed in a circulated oil bath as shown in Figure 30, although accumulation of heavy product upstream of the catalyst bed led instead to insertion of the reactor tube inside an electric furnace. The reactor tube was held in position by the use of 1 1/4 o.d. steel spacers, resulting in more uniform temperature control.

As shown in Figure 28, the catalyst was retained in the reactor between aluminum insulation. Glass wool was unsatisfactory, since the fineness of the catalyst sample, 200/325, resulted in loss of the catalyst. The catalyst was mixed with an equal weight of ground glass powder, -50 + 100 mesh. The glass powder was used to prevent agglomeration of the catalyst into a hard pellet, behavior that had been observed in trial runs. A chromel-alumel thermocouple was inserted into the reactor tube so that the thermocouple tip was in contact with the catalyst bed.

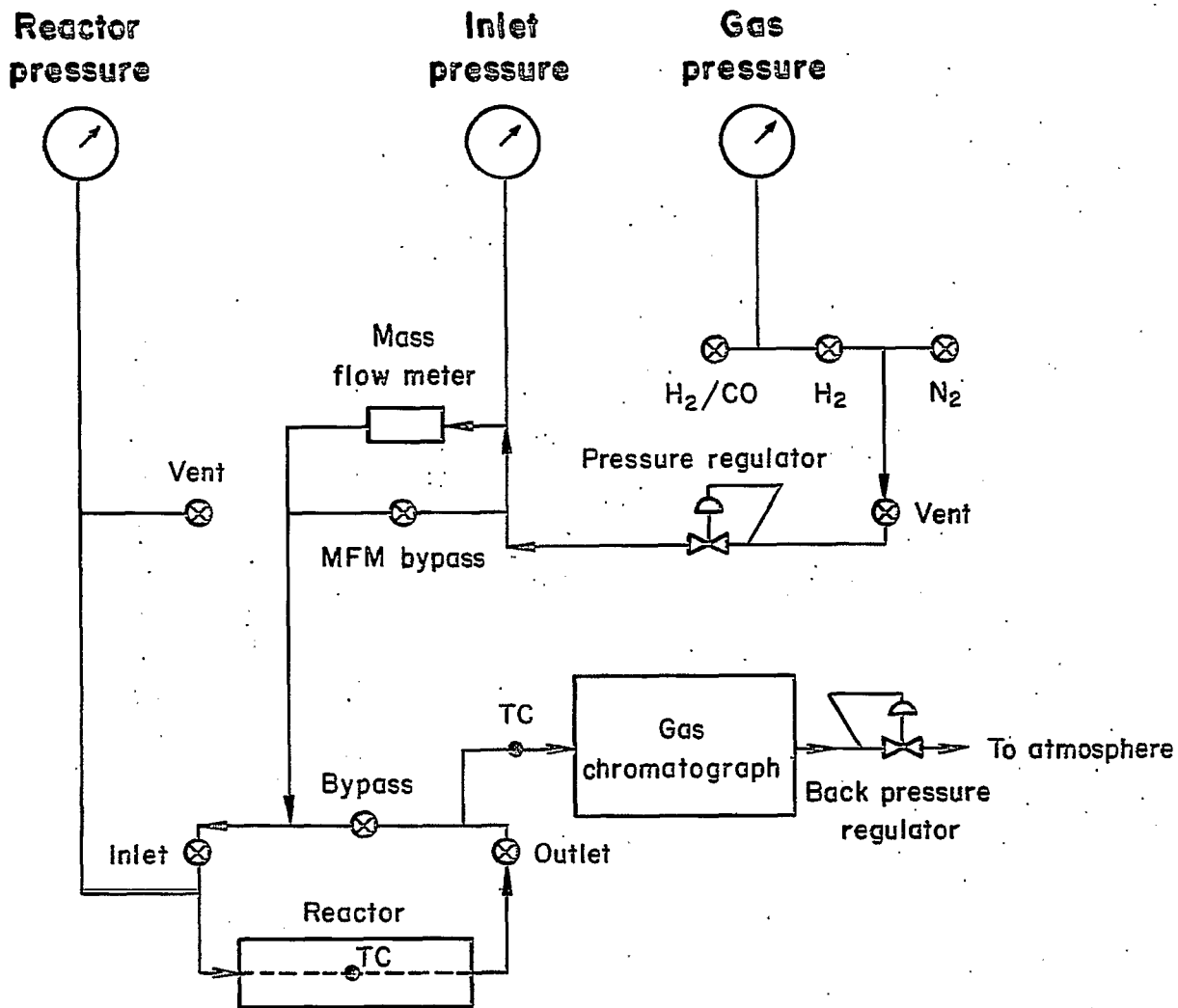


Figure 27 - Micro reactor unit

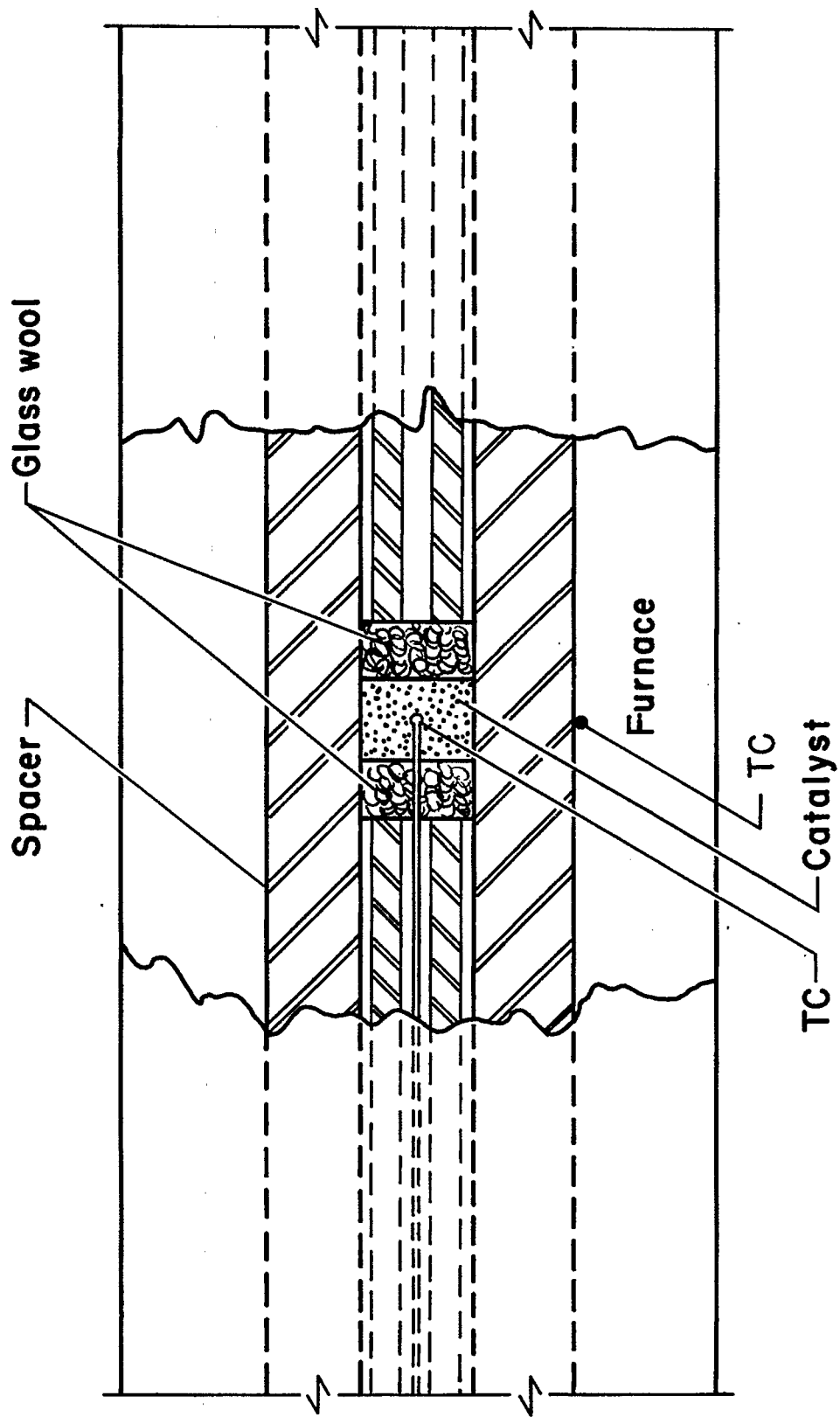


Figure 28 - Reactor

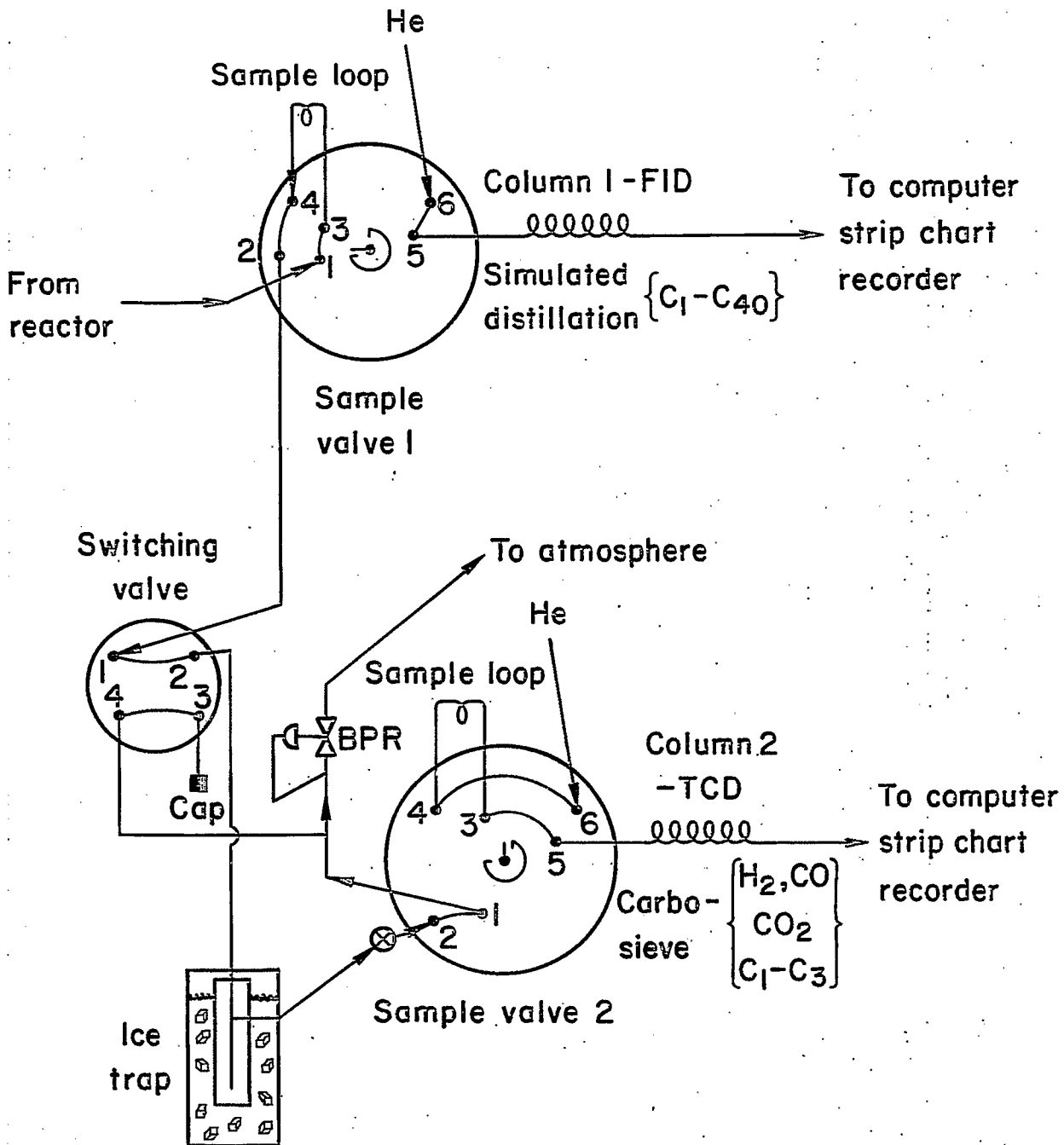
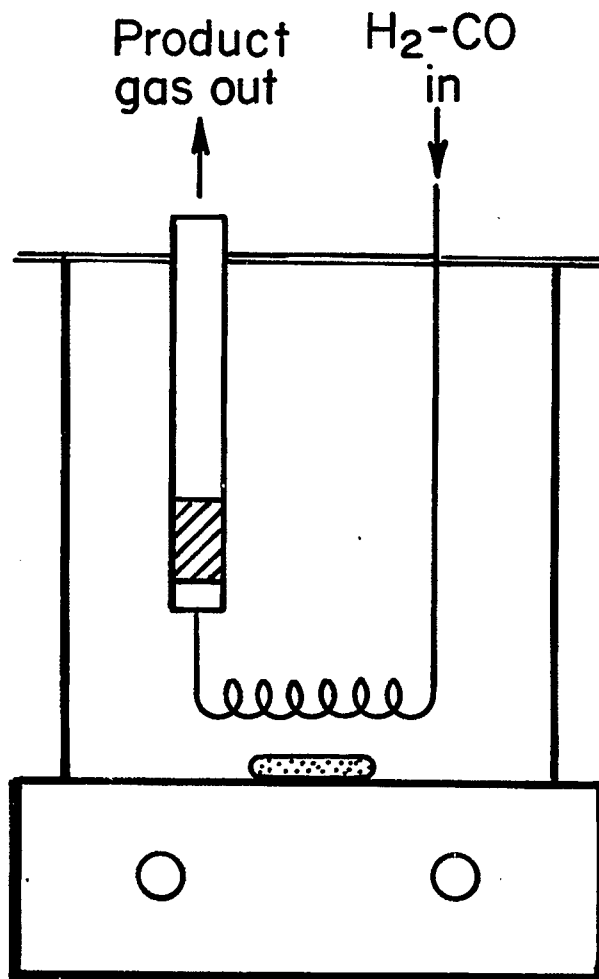


Figure 29 - Gas chromatograph



Magnetic stirrer hot plate

Figure 30 - Synthesis gas reaction unit .

After placing the catalyst in the reactor, and locating the reactor in the furnace, the reactor was heated to a given temperature with hydrogen flowing through it at 60 mL/min. Reduction was carried out at atmospheric pressure for a specified period of time, usually two hours.

When carbiding the catalyst, the temperature was reduced to 240°C in hydrogen. Carbon monoxide was then introduced at 60 mL/min and carbiding proceeded at atmospheric pressure for one hour. When preparing nitrided catalysts, the reactor temperature, after reduction, was lowered to 350°C. Ammonia was then admitted at 100 mL/min for one hour at atmospheric pressure. After nitridding or carbiding had been completed, H₂ + CO synthesis gas was admitted to the reactor unit at a rate of 100 mL/min until reaction pressure of 300 psig was reached; then the flow rate was decreased to 30 or 60 mL/min.

A Hewlett-Packard 5730A gas chromatograph equipped with dual FID and dual TCD capabilities was used for on-line analysis. The columns were a 20" x 1/8", 10 % SP2100 on 100/120 Supelcoport for detecting hydrocarbons and a 7" x 1/8", 100/120 Carbosieve 5 column for detecting carbon monoxide, carbon dioxide, and light hydrocarbons. Sample introduction was performed by means of two sample loops of 0.125 mL for the carbosieve column and 0.250 mL for the SP2100 column. The data was recorded graphically on a dual-pen strip chart recorder and onto a computer through a 2 A/D converters. The flow rates were 30 mL/min for helium (carrier gas), 60 mL/min for hydrogen, and 240 mL/min for air. The injection port and sample loops were heated to 300°C, and both detectors were also set at 300°C. The oven was temperature programmed beginning at -50°C, with a hold time of 2 minutes. The oven temperature was then increased at a rate of 8°C/min until 300°C was reached. The oven was held at 290°C for 32 min. Response factors were determined by standard methods.

Catalyst tests were continuous, with both gaseous and liquid product samples being taken every 24 hours. Gaseous components were analyzed using gas chromatography while liquid samples were analyzed using simulated distillation and functional groups were determined using infrared spectrometry. The percent conversion was defined as follows:

$$\% \text{ conversion} = \frac{\text{grams of carbon as hydrocarbons exiting reactor}}{\text{grams of carbon as CO entering reactor}} \times 100$$

$$\text{Selectivity (C}_{5+}\text{)} = \frac{\text{grams of C}_{5+}}{\text{grams of hydrocarbon product}} \times 100$$

$$\text{Carbon balance} = \frac{\text{grams of carbon as hydrocarbons, CO}_2, \text{ and oxygenates exiting reactor}}{\text{grams of carbon as CO entering reactor}}$$

Simulated distillation --- percentage of C₅₊ product with a boiling point less than 400°F.

Space velocity = Liters syn gas per hour per gram catalyst

SATISFACTION GUARANTEED

NTIS strives to provide quality products, reliable service, and fast delivery. Please contact us for a replacement within 30 days if the item you receive is defective or if we have made an error in filling your order.

▲ **E-mail: info@ntis.gov**

▲ **Phone: 1-888-584-8332 or (703)605-6050**

Reproduced by NTIS

National Technical Information Service
Springfield, VA 22161

This report was printed specifically for your order from nearly 3 million titles available in our collection.

For economy and efficiency, NTIS does not maintain stock of its vast collection of technical reports. Rather, most documents are custom reproduced for each order. Documents that are not in electronic format are reproduced from master archival copies and are the best possible reproductions available.

Occasionally, older master materials may reproduce portions of documents that are not fully legible. If you have questions concerning this document or any order you have placed with NTIS, please call our Customer Service Department at (703) 605-6050.

About NTIS

NTIS collects scientific, technical, engineering, and related business information – then organizes, maintains, and disseminates that information in a variety of formats – including electronic download, online access, CD-ROM, magnetic tape, diskette, multimedia, microfiche and paper.

The NTIS collection of nearly 3 million titles includes reports describing research conducted or sponsored by federal agencies and their contractors; statistical and business information; U.S. military publications; multimedia training products; computer software and electronic databases developed by federal agencies; and technical reports prepared by research organizations worldwide.

For more information about NTIS, visit our Web site at <http://www.ntis.gov>.

NTIS

**Ensuring Permanent, Easy Access to
U.S. Government Information Assets**



U.S. DEPARTMENT OF COMMERCE
Technology Administration
National Technical Information Service
Springfield, VA 22161 (703) 605-6000
